PB 205 188

ELECTRICAL INDUCTION OF PARTICULATE AGGLOMERATION

BY

J. R. Melcher & K. S. Sachar

Final Report under Task #7

Contract #68-002-0018

August 10, 1971

Reproduced by
NATIONAL TECHNICAL
INFORMATION SERVICE
Springfield, Va. 22151

ELECTRICAL INDUCTION OF PARTICULATE AGGLOMERATION

BY

J. R. Melcher & K. S. Sachar

Final Report under Task #7

Contract #68-002-0018

August 10, 1971

Attention:

Mr. Robert C. Lorentz
Air Pollution Control Office
Mutual Plaza, Annex 411
411 W. Chapel Hill St.,
Durham, No. Carolina 27701

126-2

BIBLIOGRAPHIC DATA SHEET	1. Report No. APTD-0869	2.	3. Recipient's Accession No.
4. Title and Subtitle Electrical Induction of Particulate Agglomeration			5. Report Date August 10, 1971 6.
7. Author(s) J. R. Melcher and K. S. Sachar			8. Performing Organization Rept. No.
9. Performing Organization Name and Address Massachusetts Institute of Technology Department of Electrical Engineering Continuum Electromechanics Group Cambridge, Massachusetts 02139			10. Project/Task/Work Unit No. Task # 7 11. Contract/Grant No. 68-002--018
12. Sponsoring Organization Name and Address Air Pollution Control Office Mutual Plaza, Annex 411 Durham, North Carolina 27701			13. Type of Report & Period Covered Final 14.

15. Supplementary Notes DISCLAIMER: This report was furnished to the Air Pollution Control Office, Durham, North Carolina, in fulfillment of Contract No. 68-002-0018.

16. Abstracts

A report is presented of a project dealing with the role of electric fields in agglomeration processes. The objectives in this preliminary feasibility study relate to agglomeration characterized as follows: (1) the gas-entrained particulate includes particles of both signs, so that charge neutrality on the macroscale is preserved; (2) two families of particle sizes are used. It is agglomeration between fine particulate and large particles that is of interest through the microfields existing between these particles. The task objectives for the project are as follows: (1) provide theoretical estimates of the feasibility of using the agglomeration process described above, in a practical conditioning device; (2) to glean what evidence there is from the literature that such agglomerative interactions occur; (3) to make preliminary experimental tests to demonstrate the type of agglomeration of interest.

17. Key Words and Document Analysis. 17a. Descriptors

Air pollution
Atmosphere contamination control
Particles
Agglomeration
Feasibility
Electric charge
Flue gases
Particle size

17b. Identifiers/Open-Ended Terms

Particulates
Air pollution control

17c. COSATI Field/Group 13B, 20I

18. Availability Statement	19. Security Class (This Report)	21. No. of Pages
Unlimited	UNCLASSIFIED	68
	20. Security Class (This Page) UNCLASSIFIED	22. Price

FORM NTIS-35 (10-70) USCOMM-DC 40329-P71

TABLE OF CONTENTS

	Pg. No.
I. Objectives	1
A. Introduction	1
B. Description of a Class of Devices	2
C. Task Objectives	8
II. Background	9
A. Agglomeration Through Interactions at Walls	10
B. Field Observations Related to Electrically-Induced Agglomeration	12
C. Supporting Theoretical and Experimental Investigation	13
III. A Systems Model for an Agglomerator	15
A. Purpose of the Model	5
B. Charging Section	16
C. Mixing Section	17
D. The Agglomerating Section	20
1. Theory of Cross-Spectrum Agglomeration Process	20
2. Representation in Terms of Discrete Spectra	23
3. Two-Family Idealization of Agglomeration Process	25
E. Agglomerator Systems	29
1. Series Staging	30
2. Particle Feedback for Improved Efficiency	32
F. Numerical Studies and Examples	34
IV. Experimental Studies	38
A. Experimental Objectives	38
B. Preliminary Observations	38

Table of Contents, (continued)

C. Oil-fired Experiment: Test Facility 41

D. Oil-fired Experiment: General Observations 43

E. Pre-agglomeration at the Charging Section Surfaces 47

F. Volume Agglomeration in the Drift Zone 53

V. Summary Remarks and Conclusions 60

Appendix 62

References 63

I. Objectives

A. Introduction

Devices used for removal of particulate from gases typically show a dramatic loss in efficiency for particles below about 1μ in size [1]. It is natural to approach the problem of their removal by taking advantage of mechanisms that tend to make the fine particles agglomerate, and hence reach sufficient proportions that they can be removed through conventional means.

As the brief review of related work in the next section illustrates, there are many mechanisms by which agglomeration or coagulation between particles in a gas can occur. Of these, a number involve the forces resulting from particle charges, hence are described as being "electrically-induced agglomeration". However, both in terms of the basic physical mechanisms and the practical implications, there are essential differences between approaches to making use of electric fields in controlling agglomeration.

It is easiest to delineate those features of the present work that distinguish it from other approaches if a schematic description of a class of devices is given at the outset. So, to clarify our objectives, we first describe briefly the agglomerator device in schematic terms, then point out features of the interaction that are a departure from previously taken approaches, and make a summary statement of objectives.

B. Description of a Class of Devices

The mixture of large and small particles (the dirty gas) enters a prototype section from the left, as shown schematically in Fig. I.1. In the charging section, all sizes are charged in a manner that insures oppositely charged particles distributed throughout the size range. This can be done in many ways.

Two direct approaches use corona sources: (a) the corona wires are driven by alternating voltage, so that they charge particles in their vicinity positively and negatively as they stream by. The result is a traveling wave of charge immediately following a given wire. The homogeneous system of charged particles is achieved by mixing in the region just downstream; wires are driven alternately out of phase, so that mixing is augmented by cross-streaming of gas between regions downstream of neighboring charging wires; (b) wires are alternately maintained at positive and negative dc potentials. Thus, a stream of particles having the same sign of charge emanates from a given wire, but is mixed with the streams from the oppositely charged neighbors as the gas passes through the mixing region.

If the particulate is relatively conducting, an indirect means of obtaining oppositely charged families of particles makes use of a corona source to charge all particles to one polarity, and then passes the particles between conducting electrodes having a potential difference. With the drift velocity caused by the field across the flow comparable to the gas velocity, the particles travel between the plates several times. With each contact at an electrode, the charge is reversed, with the result that particles leave the region between the plates with both polarities. Since, in view of the adhesive properties of the particulate, it will tend to

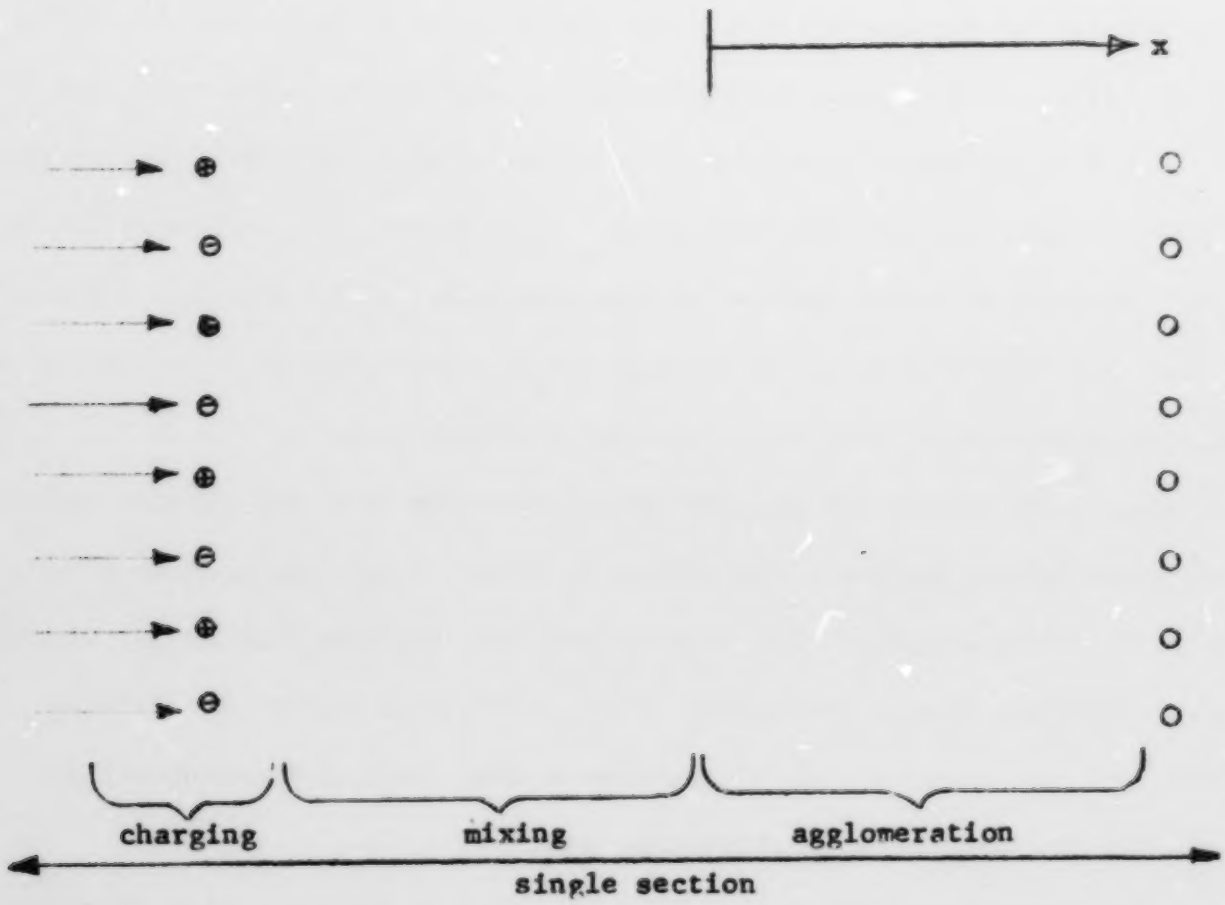

Figure I.1 Schematic representation of agglomeration system

leave the electrode in the form of agglomerates, this charging mechanism is likely to be closely connected with the creation of particle families which have widely differing size ranges. The existence of large particles is essential to the agglomeration mechanism of interest here. A more detailed description of this type of charging section in given in § IV.E.

Once the charged particles have become mixed, and hence essentially neutral, conditions are obtained at the macroscale - the agglomeration process caused by relative motions of the particles at the microscale takes place. For convenience, this process can be envisioned as occurring in an agglomeration region following the mixing region shown in Fig. I.1. Actually, both mixing and agglomeration can occur in a distributed fashion throughout these regions. The mixing is likely to predominate at first, the agglomeration later. The regions are not distinguished by any electrode structures, but rather are simply drift regions occupied by the flowing dirty gas. It is this lack of components that makes the agglomeration mechanism proposed here an attractive one.

For purposes of discussion, suppose that we define a size distribution function for the particulate $f(\bar{r},a,t)$, where $\bar{r}$ is the position in space, a is the particle "radius", and t is the time. The number density of particles in the radius range a to a + da at the position $\bar{r}$ and time t, is

$$f(a)da \quad \text{particles/unit volume} \tag{I.1}$$

Typically, the particle distribution function might depend on size, as sketched below in Fig. I.2.

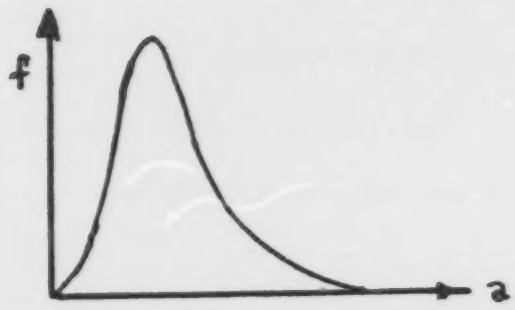

(a) Natural distribution for typical dirty gas

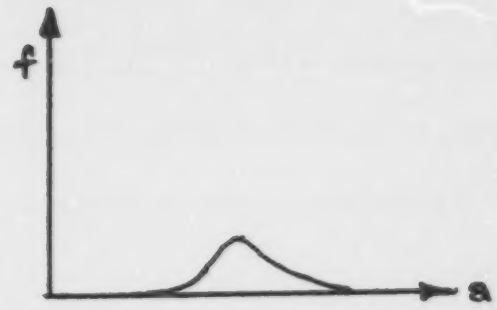

(b) Desirable skewing of distribution toward higher particle size

Fig. I.2 Distribution functions as they might depend on particle radius.

Our object is a device which tends to attenuate the particle population at low radii by achieving attachment of the particles to larger ones. Hence, the distribution function is skewed toward the higher radii. Note that the decrease in numbers at low (a) could be dramatic without much of an increase in f at large radii: the attachment of a large number of small particles to a larger particle would result in relatively little shift to the right in the larger particle range.

The advantage of agglomeration between large and small particles is the large increase in effective size of the small particles achieved in a single encounter. Particles themselves are the collection sites for smaller particles, much as the electrodes are conventionally the collection sites in a precipitator. In such a device, the larger particles are essential, and hence must not be precipitated. By contrast with the conventional precipitation approach, wherein the small particles are the last to be removed, here the smallest particles are reduced in population first. Hence,

the device agglomerates small particles onto larger ones as a conditioning process, prior to filtration by conventional techniques: electrostatic precipitators, cyclones, etc. The contrast between scaling for the agglomerator and a conventional precipitator is illustrated as follows.

Consider conventional particle precipitation to the walls of a tube or conduit having cross-sectional area A and precipitating perimeter S. If there are n particles per unit volume of the particulate to be collected, and the electrically-induced radial velocity at the precipitation wall is taken as w (the product of the particulate mobility b and the radial electric field intensity at the wall), then the schematic one-dimensional model represented in Fig. I.3 can be used to deduce the expression for steady-state precipitation

$$AUdn = - Swndx \qquad (I.2)$$

where U is the mean (of the turbulent) flow velocity.

With the assumption that w is independent of x, and hence not influenced by n, for example, we see from Eq. (I.2) that the particle density decays with distance at a rate typified by the decay length ℓ_n

$$\ell_n \equiv \frac{UA}{Sw} \quad . \qquad (I.3)$$

The smaller w, the greater the decay length ℓ_n, and therefore the greater the tube length required to achieve a given removal of the particulate. By contrast, consider now particle surfaces used to replace the collection electrode surfaces. A decay length analogous to that given by

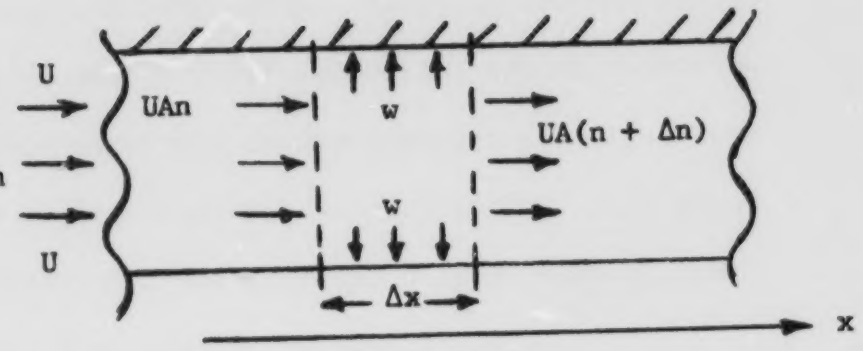

Fig. I.3 Schematic view of conventional precipitation section

---

Eq. (I.3) can be defined. If we think of the collection particles (having radius R, number density N, and charge such that their surface electric field is E_p) as being sites tantamount to removal of the particulate (having density n and mobility b), then the particulate collected by a single collecting particle per unit time is $4\pi R^2 bE_p n$ and NAdx times this quantity is the total particulate number collected in the distance dx. Instead of Eq. (I.2), we then have

$$dn = -\frac{ndx}{\ell_p} \quad ; \quad \ell_p = \frac{U}{4\pi R^2 NbE_p} \quad . \tag{I.4}$$

A test of the advantages inherent in using the particles as collection sites, rather than walls, is made by comparing ℓ_p and ℓ_w. If we define E_w as the electric field at the wall of the conventional precipitator, then $w = bE_w$, and the ratio of collection lengths is

$$\frac{\ell_p}{\ell_w} = \frac{S/A}{4\pi R^2 N} \frac{E_w}{E_p} \quad . \tag{I.5}$$

The surface-to-volume ratio of the conventional precipitator collection channel is S/A. Becuase $4\pi R^2 N$ is the surface-to-volume ratio of the collecting particles, we see from Eq. (I.5) that any advantage obtained from using particles as collection sites comes from having a high relative

surface-to-volume ratio. Note, however, that there is an additional advantage if the collecting field E_p can be made large compared to that practical in a conventional precipitator collection channel. It is well known that dielectric breakdown strength of a gas is increased if the field is concentrated around a small particle.

Although the simple model used to introduce the fundamental ideas in this section gives no clue as to how the particles are to be used effectively as collection sites, it does illustrate that a new type of scaling is introduced. The collection of ultra-small particulate takes place in a region occupied by the system of particles; no electrodes are required. But, to be efficient, a population of collecting sites must be maintained. Large sized particles are desirable, and should not be removed until after the small particulate has been collected.

C. Task Objectives

It is recognized that electric fields play a part in a wide range of agglomerative processes. Some of these are reviewed and related to this project in Section II. Our objectives in this preliminary feasibility study relate to agglomeration characterized as follows:

1. The gas-entrained particulate includes particles of both signs, so that charge neutrality on the macroscale is preserved. This means that, in the scaling of devices, there is no tendency of a macrofield to increase with increasing volume-to-surface ratio.

2. Two families of particle sizes are used. It is agglomeration between fine particulate and large particles that is of interest through the micro-fields existing between these particles.

Objectives are:

1. To provide theoretical estimates of the feasibility of using the agglomeration process described above in a practical conditioning device.

2. To glean what evidence there is from the literature that such agglomerative interactions occur. Here, we refer not only to basic studies, but to descriptions of field tests that have implications for the process of interest.

3. To make preliminary experimental tests to demonstrate the type of agglomeration of interest. Here, no attempt is made to deal with submicron particles, but rather, feasibility is based on interactions between fine particles in the μ range and large particles in the 10-100μ range. These preliminary experiments are conducted to demonstrate engineering feasibility, and hence detailed control of particle size, charge, etc. and the attendant quantitative insights are sacrificed for realistic operating conditions, and hence generally qualitative results.

II. Background

In any agglomerative process, there are two basic considerations; the means by which particles encounter each other, and the mechanism by which they adhere once in contact. Both of these considerations are influenced by particle charging. Our investigation is primarily concerned with mechanisms that lead to the initial contact. Nevertheless, there is no opportunity to observe the agglomeration unless particles adhere, and certainly practical applications will result only if the adhesion of particles is sufficient to sustain the agglomeration until the particles are removed from the system. In the following, we emphasize the process by which the particles come together, and that will be referred to as the "agglomeration process". Of the many physical parameters that influence adhesion, only those that allow a demonstration of the agglomeration are of interest here.

A. Agglomeration Through Interactions at Walls

Much of what is found in the literature pertaining to "electrically-induced agglomeration" is related only indirectly to the "bulk" agglomeration of interest in this investigation. A single-stage precipitator of essentially conventional design can act as an agglomerator. Particles, charged by a coaxial corona wire and collecting electrode, are precipitated until they form a sufficient thickness to be re-entrained, either through aerodynamic drag forces or because of the reversal in electric force that accompanies the exchange of charge between particles and wall upon contact. The re-entrained particles adhere to each other because of contact at the walls, and tend to form agglomerates with sizes far larger than that of the original particles. The walls are the sites of the agglomeration.

Industrial application of the agglomeration at walls is common in dealing with particles of relatively high electrical conductivity and which have the properties required for good adhesion. For example, in the production of carbon black [2,3] submicron-sized particles of fume or smoke are removed by combinations of electrostatic precipitators and cyclone or bag-type filters. Only a small percentage of the carbon black is actually removed by means of the electrostatic precipitator. Rather, particles precipitated on the walls are apparently re-entrained in an agglomerated form, so that the electrostatic precipitator performs the function of agglomerating the particles, rather than actually removing them from the gas flow. Typically, the black is formed by the combustion of petroleum products, and hence the technique has implication for particle clearance from the oil-fired utilities installations. Note that, in the wall-type agglomerator, the coagulation occurs in a large ambient (macroscopic) electric field which is responsible for the initial particle contact with the wall.

Some work has been done to design wall-type electric agglomerators, and hence provide a quantitative model. An example is given in [5], Walker's discussion relating to commercial techniques for recovering chemical in the form of submicron fume from organic solids. There, the approach is to agglomerate the particles before using conventional scrubbing techniques. The device is envisioned as one in which the electrostatically-induced agglomeration occurs at the walls, with clear implications for the manner in which the effect scales with respect to size of a device. In connection with a pilot plant installed on a pulp mill recovery boiler in West Virginia, reasonable prediction of scrubber efficiency, including the pre-agglomeration prior to scrubbing, is made using the model. In the analytical model, the agglomerator is viewed as a conventional precipitator, with particle collection at the wall tantamount to particle agglomeration. Because the agglomerates are of sizes several orders of magnitude larger than the original particles, there is no necessity for bringing in the detail of the agglomeration to larger sizes. This work supports the contention that electrostatic pre-agglomeration by means of coagulation at walls materially influences the performance of inertial scrubbers used to remove particulate. Walker's work also emphasizes the necessity for having conditions of temperature, humidity, etc., favorable to the formation of stable agglomerates.

A somewhat different configuration for achieving wall agglomeration is described in two patents [6,7] and sketched in Fig. II.1. The device is contained by a cylindrical shell, and consists of a ceramic block with flues or channels extending through it, as shown in the half-section in Fig. II.1a and in end view in Fig. II.1b. In alternate flues, there are

electrodes supported from opposite ends of the block. One distinguishing feature of the configuration is the use of the non-metallic walls. Another is that the voltage applied between the electrodes is alternating. It is presumed from the patent description that particles collect at the walls and are re-entrained in the form of agglomerates.

The reason for using the insulating walls is likely to be that the particles are then prevented from reversing their charge upon contact with the surface, and being repelled back into the flow. This same reasoning is applied in § IV to explain the enhanced collection efficiency of electrodes coated with insulation and used to indicate the bipolar charging of particulate.

B. Field Observations Related to Electrically-Induced Agglomeration

An ac precipitator having electrodes with insulating coverings has been operated with some success in dealing with highly insulating particles [8]. Aside from the obvious connection between this work and that described at the end of the previous section, the authors incidentally make an observation relevant to agglomeration, this time using products of coal combustion. The precipitated particles are observed to be coarse compared to particles precipitated by a dc voltage. Here, there is some implication for the idea of using oppositely charged particles to achieve agglomeration, because in the ac field, particles of both signs are present.

In an article bearing clear testimony to the existence of electrostatically induced agglomeration under field conditions, Szantho [9] describes tests done on a practical facility incorporating a conventional electrostatic precipitator and the products of coal combustion. Measurements determine the site of agglomeration evident in the emissions from a stack. The author attributes the enhanced agglomeration to bipolar

charging, and hence the phenomenon is represented as relevant to the agglomeration of interest here. Because the agglomerants coming from the electrostatic precipitator are effectively reduced in size by a subsequent head draft, the agglomeration process is felt to occur mainly beyond the electrostatic precipitator. The degree of agglomeration is found to depend upon the type of coal fired; there seems to be a correlation between high ash content in the fuel and the observed agglomeration. Although the author did not attribute this to differences in the adhesion of particles resulting from burning various types of coal, it is clear that his investigations demonstrate that cohesive forces on coal products at practical operating temperatures can be sufficient to sustain the coagulation, once the collision between particles is obtained.

It is not clear from Szantho's work whether agglomeration occurs because of impacts between particles at the walls, or in the volume. Significantly, it does appear to occur in regions where a macroscopic electric field is absent. Moreover, it is found that agglomeration is enhanced in those regions of high fluid turbulence. The author seems to feel that agglomeration is caused by a "bi-ionization", or in other words, electrostatic attraction between particles of differing charge polarity. His experimental evidence to support this contention is at best, however, partial; his explanations must be regarded as plausibility arguments.

C. Supporting Theoretical and Experimental Investigations

In reviewing the literature of agglomeration induced by particle charging, it is important to distinguish between processes exploiting micro and macro fields. For example, particles in a macroscopic (ambient)

electric field imposed, say, by means of external electrodes are generally polarized, and the resulting distortion of the electric field is the basis for electrical forces between particles [10]. Such dipole interactions are not of interest here because, except for the rare cases of ferroelectric materials, they are created only by an ambient field.

Similarly, those effects resulting because the particulate has a net charge are not of interest here [11]. Rather, literature relating to agglomeration when the particulate is charged in a bipolar manner is of interest. The aging of smokes [12] is thought by some [13] to be influenced by natural particle charging. Most studies of agglomeration and coagulation relate to interactions between particles having approximately the same size. Gillespie's work [13] is an example in which connection between bipolar charging and coagulation is observed. Two types of particles are used in the related studies reported by Zessack [14]. Although these coagulation experiments and their supporting theoretical developments relate to the type of agglomeration of interest here, they do not pertain directly to the agglomeration induced by fields between particles which are greatly disparate in size. They do illustrate that the adhesive forces necessary for exploiting agglomeration are found in a wide range of circumstances.

The experiments reported by Kraemer and Johnstone [11] do give direct support to the agglomeration model used extensively in the next section. These authors report the collection efficiency of a charged metallic spherical "particle" placed in the flow of a charged aerosol. Several collection mechanisms not of interest here are discussed. For example, with a unipolar charging of the aerosol, there is collection, even with

the sphere uncharged, because of the fields due to the charge on the fine particles. This mechanism is not present if the fine particles are charged in a bipolar manner. However, for their studies in regard to collection on a charged sphere with effects of the unipolar aerosol charging negligible, an encouraging correlation is found with essentially the same collection model used in § III.D.

III. A Systems Model for an Agglomerator

A. Purpose of the Model

The schematic representation of the agglomerator device given with Fig. I-1 helps in separating the fundamental issues. Our main interest is in the agglomeration section. Nevertheless, the success of the approach hinges on obtaining the required bipolar charging and the maintenance of particle families differing considerably in size. In the next two sections, preliminary factors concerned with the charging and mixing are discussed. In Chapter IV, further discussion of charging is necessary, since it is found in experiments that particle charging, creation of two particle families, and mixing can be accomplished with a single corona charger.

Most of this section is devoted to developing design equations for an agglomerator section, regardless of the charging process. The objective is a self-consistent model for the simultaneous skewing of the size distribution function and discharging of the collection family of particles. By restricting the model to a simple impact collection process (strictly valid only for micron-sized particles or larger), it is possible to provide a complete description of the system. Thus, improvements in performance caused by staging and feedback of particles can be developed; this is done in § III.E.

B. Charging Section

The charging section can exploit conventional physical processes. Ions generated by corona discharge on the wires in the charging section drift through the region traversed by the particles, and hence charge the particles, either diffusively or by impact. The particles having sizes greater than about 0.5 μm are charged by impact, while those that are smaller are charged by diffusion. The important point is that bipolar charging be achieved. Hence, if corona charging is used, particles are given a monopolar charge and must be mixed with particles of opposite sign in some other region.

Other means of charging will be discussed in detail in § IV.E . But as a preview, if the collection particles are electrically conducting, an optional mode of charging would be to use charge induction as the particles make contact with an electrode. As might be inferred from this, the full useful application of the electrostatic agglomeration concept is not explored until the possibility of injecting additional particles, or of feeding back selected particles for the collection function, is investigated.

To provide a first estimate of the agglomerator performance, we require the dependence of particle charge on particle radius, a. If we assume that the effective charging field in the corona region is E_o, then an impact-charging model leads to a charge-per-particle that quickly saturates at the value

$$q(a) = 12\ \pi\varepsilon_o a^2 E_o \quad . \tag{III.1}$$

Hence, with the assumption that E_o is set by the charging section arrangement and voltage, Eq. (III.1) gives the charge dependence on radius at the inlet to the mixing region. Note that, once the particles have been mixed, there is no macroscopic field. The effective collection field is that at the particle surface. For the charge given by Eq. (III.1), that field is

simply

$$E_p = \frac{q(\bar{r},a,t)}{4\ \pi\varepsilon_o a^2} \quad ; \quad q(\bar{r}_c,a,t) = 12\ \pi\varepsilon_o a^2 E_o \ . \qquad \text{(III.2)}$$

where $\bar{r}_c$ signifies the position of the charging saturation. In what follows, we will assume that the mixing section is crossed by the particles without decay of this saturation charge, so that $\bar{r}_c$ is the plane x = 0 at the inlet of the agglomeration section. Any agglomeration in the mixing region would tend to increase the effectiveness of the device. The following might be considered a worst-case analysis in that respect.

C. Mixing Section

It may not be possible actually to isolate a physical region in which mixing takes place to the exclusion of charging or agglomeration. A separate region is indicated in Fig. I.1 to emphasize the requirement for the mixing, wherever it actually obtains. For the agglomeration of interest here to take place, the gas-entrained particulate must be composed of essentially four families of thoroughly mixed particles. These are the large and small particles charged to both polarities.

As an example, with the corona charging sections described in § I.A, unipolar charging is achieved in separate regions, and it is essential that mixing be implemented before the desired agglomeration mechanism can be significant. Consider the natural mixing accompanying the oppositely charged corona wires placed across the flow.

If the gas stream is operated at a large enough Reynolds' number (Re = Ud/ν > 50, where d is the wire diameter), a vortex sheet will be established at each cylinder (see Fig. III.1). The alternately positive and negative vortices will tend to mix the fluid to a certain degree.

However, assuming that the wire voltages are driven sinusoidally at line frequency, the distance downstream over which the charge changes sign is considerably larger than the scale of eddies. For a 10 m/sec flow, the former will be $\lambda = u/f = 0.167$ m, and for a wire with 10^{-3} m diameter, the latter will be on the order of a few millimeters. Thus, this mechanism alone will not produce a zero net charge distribution.

Consider the fact, though, that the width of the wake increases in proportion to $\sqrt{x}$, where x is the downstream distance from a wire. That is, $b/d = \sqrt{x/d}$, where d is the wire diameter. The wakes from the two neighboring wires will intersect each other when $b = D$, with D the wire spacing. Since the voltages of the neighboring wires will be 180° out of phase, with either ac or dc excitation, the mixing initiated at this point should tend to decrease the net charge distribution. By the time that the flow reaches $x = 10x_o$, the mixing should be about complete. That is, the flow should have no net charge density on the scale of the most dilute particle size. Thus, for $d = 10^{-3}$ m and $D = 10^{-2}$ m (see Fig. III.2),

$$x_c = 10\, x_o = 10\left(\frac{b^2}{d^2}\, d\right) = 10\, \frac{(10^{-2})^2}{10^{-3}} = 1 \text{ m}. \qquad \text{(III.3)}$$

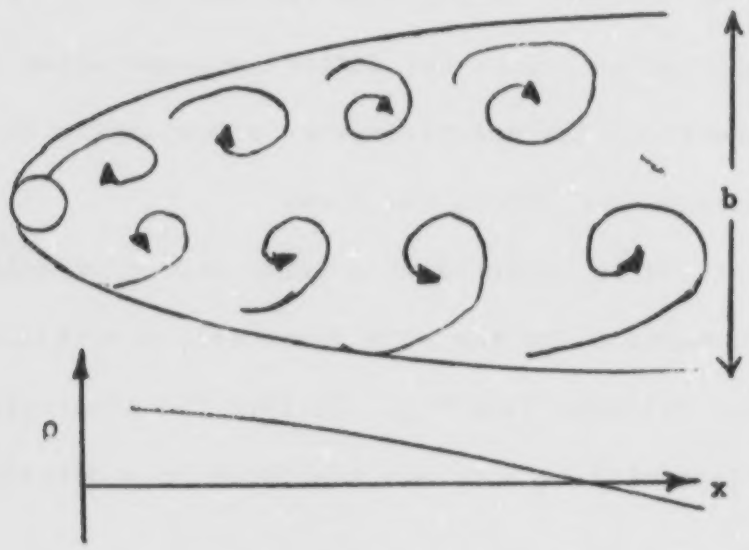

Fig. III-1 Vortex sheet and charge distribution emanating from a single wire driven by a sinusoidal voltage

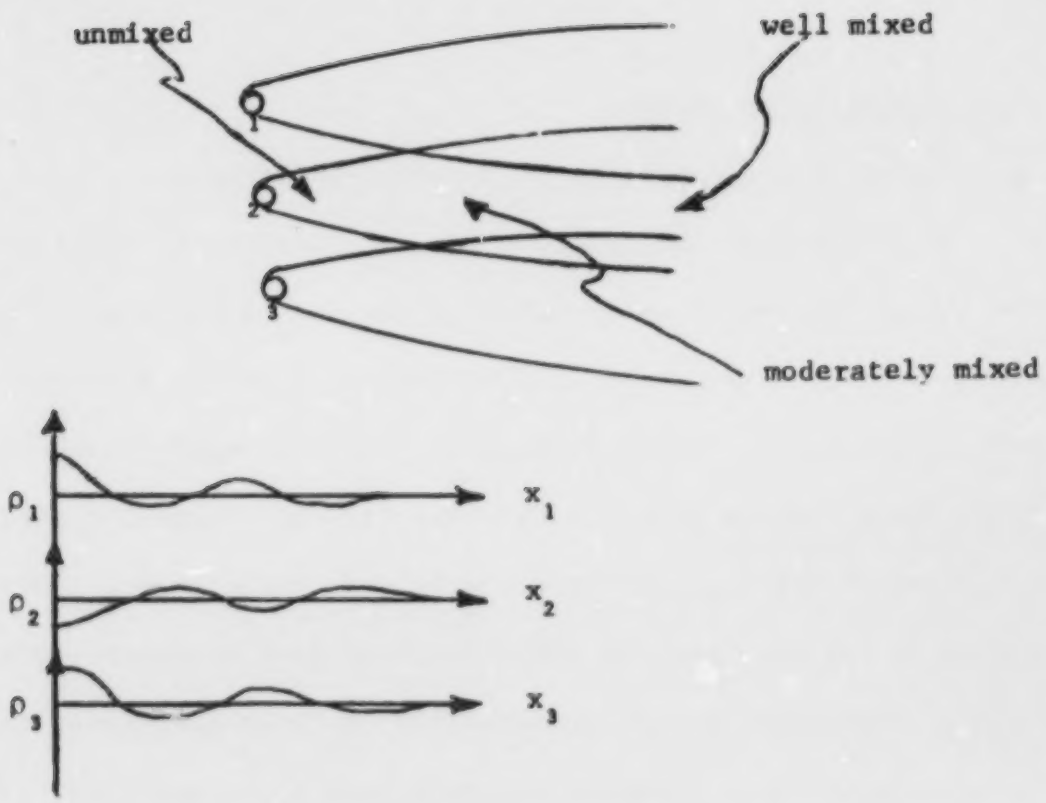

Fig. III-2 Charge distribution at one instant for superposition of vortices from several wires with sinusoidally-driven voltages.

The latter figure should be considered an upper bound on the mixing length, since the flow was considered to be initially laminar when incident on the wires. Actually, it is fairly turbulent before it even reaches the grid.

In the charging section, there is likely to be mixing due to electrohydrodynamic effects [15]. With the passage of ions and charged particles across the flow, there is an associated turbulence that can be responsible for considerable mixing. If this is taken together with the fact that charged particles created by ion impact can reach the opposite electrode and reverse their polarity, it is seen that a single corona charging section can, under suitable conditions, promote not only the desired bipolar charging, but also the required mixing. More will be said about this in § IV.E .

D. The Agglomerating Section

1. Theory of Cross-Spectrum Agglomeration Process

As outlined in the introduction, the purpose of the agglomerating section is to achieve an attenuation of the low particle size densities, as characterized by the shift in distribution function f(a) sketched in Figs. I.2a and I.2b. Hence, we wish to establish expressions that describe the distribution of $f(\bar{r},a,t)$. Because the charge per particle is also varying in the agglomeration process, we also require a description of $q(\bar{r},a,t)$. To this end, we state physical laws accounting for the migration of particles and the conservation of their associated charges.

We define a mean velocity for particles as $\bar{v}$, which for our present purposes is the gas velocity. We assume that the electrical forces have a negligible effect on the gas motion, so that $\bar{v}$ is a function of space and time determined by the flow characteristics alone. More properly, when conservation of a certain size particle with a certain sign of charge is applied to a given volume, the effects of both turbulence and the inter-particle electric fields average to zero. We can take this function as known in describing the agglomerator section. Then, conservation of the number of particles in a size range a is accounted for by

$$-\frac{\partial f\Delta a}{\partial t} = \nabla\cdot(f\Delta a\bar{v}) + S\Delta a \qquad \text{(III.4)}$$

Here, $S\Delta a$ is the number of particles per unit volume/second lost from Δa to other size ranges, minus a similar number brought in by collection from other size ranges.

A second equation is best written by considering an individual particle and requiring that its increase in charge, q, be accounted for by

the current carried by particles of the opposite sign impacting (or diffusing to) its surface.

$$\frac{Dq}{Dt} = -i \quad . \tag{III.5}$$

Actually, for each equation written for the positively charged particles of radius a, we can write its twin expression for its oppositely charged counterpart. The particles charging the one on the left-hand side of the equation are oppositely charged from it, and hence belong to the twin system. Assuming that we have succeeded in creating equal quantities of oppositely charged particles of every size, then the particle distributions of each system will be perfect images of each other.

In the following, we make the approximation that in any range of interest of the radial distribution, the number of particles leaving because of collection by larger particles greatly exceeds that coming in, because smaller particles have collected yet smaller particles, with a resulting increase in their size. Similar arguments pertain to the electrical current carried by particles as they are collected. The current collected by a single particle of radius a', due to image of particles in the size range Δa, is:

$$K\Delta a = q(a)b(a)f(a)\Delta a E_p\ (\bar{r},a',t)\ 4\pi a'^2 \tag{III.6}$$

Similarly, the number of particles/sec collected by particles having radius a' from the range Δa (per-unit volume) is

$$\Gamma\Delta a = b(a)f(a')\Delta a' E_p\ (\bar{r},a',t)\ 4\ \pi a'^2 \quad . \tag{III.7}$$

Note that $E_p = q(\bar{r},a',t)/4\pi\varepsilon_o a'^2$.

From Eq. (III.7), it follows that

$$S\Delta a = \Delta a \int_a^\infty f(a)da' \, \Gamma(a,a') \tag{III.8}$$

and from Eq. (III.6) we have the single-particle current due to all smaller impacting particles,

$$i(a') = \int_0^{a'} K(a,a')da \quad . \tag{III.9}$$

Thus, for our particular model, we have a pair of integral-differential equations governing f and q in the agglomeration section. These are obtained by inserting Eq. (III.8) and (III.7) into (III.4), to get:

$$\frac{Df(\bar{r},a,t)}{Dt} = - \frac{b(a)f(a)}{\varepsilon_o} \int_a^\infty f(a')q(a') \, da' \tag{III.10}$$

and Eqs. (III.9) and (III.6) into (III.5) to get

$$\frac{D}{Dt} q(\bar{r},a',t) = - \frac{q(a')}{\varepsilon_o} \int_0^{a'} q(a)b(a)f(a)da \quad . \tag{III.11}$$

Note that, in writing Eq. (III.10), we have assumed that the gas moves at sufficiently low velocities relative to the speed of sound, to justify setting $\nabla \cdot \bar{v} = 0$. Also, all charges are defined to be positive.

The fact that Eq. (III.10) gives f(a), while (III.11) gives q(a') serves as a reminder that, built into the model is an asymmetry concerning the interaction between large and small particles. Equation (III.10) is most meaningful if applied to the problem of finding the effect of the agglomeration on the number density of the smallest particles. Certainly the model ignores any change in the number density at the highest radii,

as can be seen either from the derivation or from interpreting Eq. (III.10). The term on the right in (III.10) is the rate of decrease for particles in the neighborhood of a fluid element of fixed identity. For values of (a) near the top of the distribution, this rate of decay vanishes. In fact, there would be a tendency for even the largest particles to increase in size, but that is ignored by the model.

Similarly, Eq. (III.11) best pertains to the decay of charge on the largest particles. Again, we can see this from the mathematical result, because if small particles are considered, the integral on the right vanishes and we conclude that the rate of decay of the particle charge at small radii vanishes. So, use is made of Eq. (III.10) to find the distribution function for the smaller particles; to do so, the term on the right couples to the larger particles through their instantaneous charge distribution. That distribution is brought in by Eq. (III.11) written for the larger particles. The formulation is then complete, because the integral on the right in Eq. (III.11) requires the particle distribution function for the smaller particles.

2. Representation in Terms of Discrete Spectra

In view of the difficulties encountered in solving the coupled integral-differential equations (III.10) and (III.11), it is convenient to approximate the continuous distribution of radii by a discrete spectrum, as shown in Fig. III.3. The continuous distribution is represented by breaking it into p discrete spectra, formally,

$$f(a) = \sum_{m=1}^{p} n_m \, u_o(a - a_m) \qquad \text{(III.12)}$$

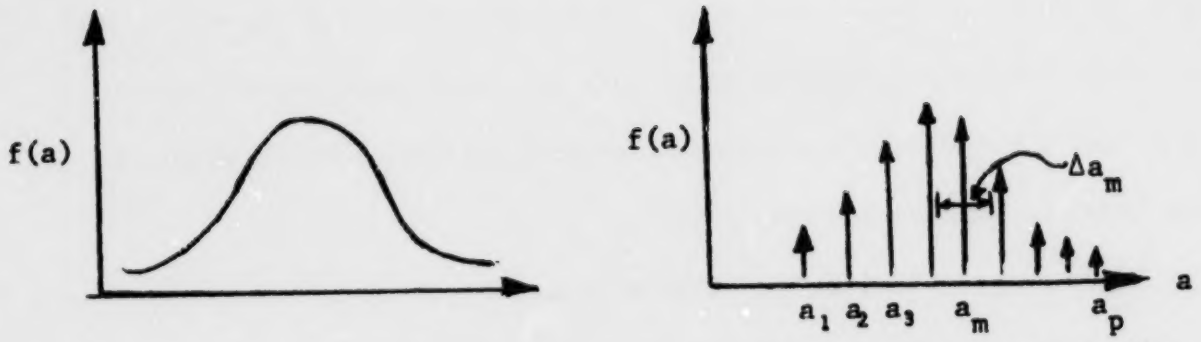

Fig. III-3 Discrete spectrum approximation used to break integral differential equations into system of coupled differential equations representing families of particles

---

where integration over the neighborhood of one impulse shows that n_m is the number density of particles within the spectral range Δa_m. We further define $q_m \equiv q(a_m)$ as the average single-particle charge over the same range, and accordingly, $b(a_m) \equiv b_m$.

For a spectral pair separated by many time the radius of the smaller range of particles, the approximation mentioned previously, of neglecting increases in particle density (at a specific radius) produced by coagulation of smaller sized particulate, becomes increasingly accurate. On substitution of the impulse train of Eq. (III.12) for the density spectrum in the coagulation and charging equations, (III.10) and (III.11), we arrive at a system of coupled differential equations,

$$\frac{Dn_n}{Dt} = \frac{-b_n n_n}{\varepsilon_o} \sum_{m=n+1}^{p} n_m q_m \quad ; \qquad n = 1 \ldots . p \tag{III.13}$$

$$\frac{Dq_n}{Dt} = \frac{-q_n}{\varepsilon_o} \sum_{m=1}^{n-1} q_m b_{mn} n_m \quad ; \quad n = 1 \ldots p \tag{III.14}$$

Thus we arrive at a representation in terms of 2p nonlinear partial differential equations.

Of greatest practical interest is the steady-state condition. If, in addition, the agglomerating geometry is essentially dependent on only the one spatial coordinate x, the system of Eqs. (III.13) and (III.14) reduces to

$$\frac{d}{dx} n_n = \frac{-b_n n_n}{\varepsilon_o U} \sum_{m=n+1}^{p} n_m q_m \quad ; \quad n = 1 \ldots p \tag{III.15}$$

$$\frac{d}{dx} q_n = \frac{-q_n}{\varepsilon_o U} \sum_{m=1}^{n-1} q_m b_{mn} n_m \quad ; \quad n = 1 \ldots p \tag{III.16}$$

where U is the mean gas velocity in the x- direction.

3. Two-Family Idealization of Agglomeration Process

To obtain both physical insight into the significance of the model and preliminary quantitative assessments of the potential of the device, we next consider the one-dimensional, steady-state system characterized by Eqs. (III.15) and (III.16). The approach also exhibits the essential nature of the particle interactions predicted by a p family set of equations, if attention is limited to the interactions of two families, a_1 and a_2, as sketched in Fig. III-4.

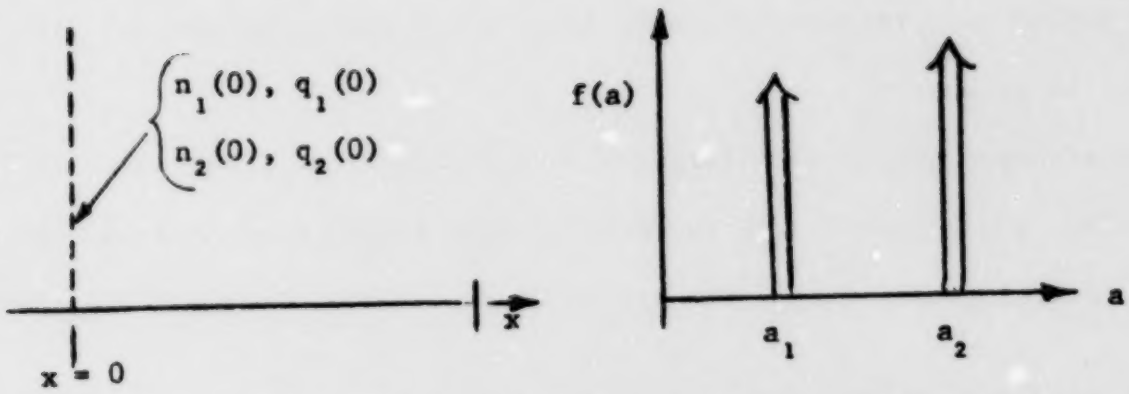

Fig. III-4 Agglomerator section performance characterized by spatial distribution of two particle families injected at x = 0 with particle densities $[n_1(0), n_2(0)]$ and charges per particle $[q_1(0), q_2(0)]$

For the present purposes, we will assume that the mobilities of both families are representable in terms of a simple Stokes' drag model,

$$b_m = \frac{q_m}{6\pi\mu a_m} \tag{III.17}$$

where μ is the gas viscosity. Then, Eqs. (III.15) and (III.16) reduce to the 2p = 4 expressions

$$\frac{dn_1}{dx} = - \frac{q_1 n_1 n_2 q_2}{6\pi\mu\varepsilon_o U a_1} \tag{III.18}$$

$$\frac{dn_2}{dx} = 0 \tag{III.19}$$

$$\frac{dq_1}{dx} = 0 \tag{III.20}$$

$$\frac{dq_2}{dx} = - \frac{q_2 q_1^{\,2} n_1}{6\pi\mu a_1 \varepsilon_o U} \tag{III.21}$$

Notice that our modeling of the system is again evident. The charge on the

smaller particles and the number density of the larger ones are predicted by Eqs. (III.19) and (III.20) to be constants: n_2 = constant and q_1 = constant. Equations (III.18) and (III.21) can then be combined and solved in terms of the inlet values $n_1(0)$ and $q_2(0)$. In the Appendix, it is shown that

$$\frac{n_1(x)}{n_1(0)} = \left\{ -\frac{1}{\eta} + \left[1 + \frac{1}{\eta}\right] e^{\eta x/\ell^*} \right\}^{-1} \qquad \text{(III.22)}$$

$$\frac{q_2(x)}{q_2(0)} = e^{\eta x/\ell^*} \left\{ -\frac{1}{\eta} + \left[1 + \frac{1}{\eta}\right] e^{\eta x/\ell^*} \right\}^{-1} \qquad \text{(III.23)}$$

where

$$\eta \equiv [(q_2(0)n_2/q_1n_1(0)) - 1] \quad \text{(loading parameter)}$$

$$\ell^* \equiv [6\pi\mu a_1 \varepsilon_o U/q_1^2 n_1(0)]$$

A useful relation between the particle density $n_1(x)$ and the charge per particle $q_2(x)$ is obtained by observing from Eqs. (III.18) and (III.21) that $\frac{1}{n_2}\frac{dn_1}{dx} = \frac{1}{q_1}\frac{dq_2}{dx}$. Because n_2 and q_1 are constants, this relation can be integrated, and the initial conditions used to show that

$$\frac{n_1(x)}{n_1(0)} = (\eta + 1)\frac{q_2(x)}{q_2(0)} - \eta \quad . \qquad \text{(III.24)}$$

Note that physically interesting values of the loading parameter range from -1 to infinity. Over this entire range, the number density and charge per particle are decreasing functions of x. However, $\eta = 0$ demarks a regime in which the charge decay limits the degree to which the

particle density is decreased from a regime in which all of the particles can be removed without completely discharging the large particles. That is, as $x \to \infty$

η	$n_1(x)/n_1(0)$	$q_2(x)/q_2(0)$	
> 0	$\to 0$	$\eta/(\eta + 1)$	(III.25)
< 0	$\to -\eta$	0	

Thus, η is an essential design parameter. If we assume that all particles are charged to saturation by the same effective field E_o in the charging section, then q_1 and $q_2(0)$ are given, respectively, by Eq. (III.1) and $q_2(0)/q_1 = a_2^2/a_1^2$. Further, $V_2/V_1 = (n_2 a_2^3)/(n_1 a_1^3)$ ... where V_2/V_1 is the ratio of total particle volumes concentrations at the inlet to the section, and we can write the loading parameter as

$$\eta = \left[\frac{a_1}{a_2}\,\frac{V_2}{V_1} - 1\right] \quad . \tag{III.26}$$

This last expression makes it clear that the price paid for being able to collect completely the smaller particles in a single section is a volume loading of $V_2/V_1 = a_2/a_1$. If particles are to be effectively changed in radius by a factor of 10 in a single stage, then the ratio of volume loadings of the large to the small particles must be in the same factor of 10. This statement uses the fact that $\eta = 0$ is the least value of the loading factor that gives a distribution of $n(x)$ approaching zero as $x \to \infty$. In fact, for $\eta = 0$, Eqs. (III.22) and (III.23) assume the simple forms

$$\frac{n_1(x)}{n_1(0)} = \frac{q_2(x)}{q_2(0)} = \frac{1}{[1 + \frac{x}{\ell^*}]} \qquad \text{(III.27)}$$

Just how rapidly the density of small particulate approaches zero in this delimiting case is clearly a function of ℓ^*. A convenient form for ℓ^* is found by making use of the charging equation, (III.1) and defining $n_1 = 1/(\alpha_1 a_1)^3$ such that α_1 is the number of particle radii a by which particles are typically spaced when they are in the number density $n_1(0)$. Then,

$$\ell^* = \frac{\alpha_1^3 \mu U}{24 \pi \varepsilon_o E_o^2} \qquad \text{(III.28)}$$

Note that this expression does not depend on the size, a_1. We can take as a typical value

$$\ell^* = \frac{(100)^3 (5 \times 10^{-5}) (5)}{(24)(\pi)(8.85 \times 10^{-12})(10^6)} \approx 3 \times 10^{-1} \text{ m} \qquad \text{(III.29)}$$

We will discuss in the next section how feedback can be used to alter this condition.

That this length is of significance similar to that illustrated in § I.B by ℓ_p is seen by noting that $b = q_1/6 \pi \mu a_1$. If we further recognize from Coulomb's law that $4 \pi R^2 E_p = q/\varepsilon_o$, it follows that ℓ_p in Eq. (I.4) can be written as $\ell_p = \varepsilon_o U/bNq$. For the particular case $\eta = 0$, we have $Nq \equiv n_2 q_2(0) = q_1 n_1(0)$, and hence $\ell_p = \varepsilon_o U/b_1 q_1 n(0)$, which is seen to be identical to ℓ^*.

E. Agglomerator Systems

For optimal use of a given volume, it is likely that agglomeration is best achieved by having several, or perhaps many, stages in series. An index as to the necessity of using series staging is the loading parameter,

η. Clearly, if η is considerably less than 0, staging is required, or only fractional clearance of the small particulate will be achieved, no matter how long the agglomeration section, But, even if η is on the order of zero, it may be desirable to use some form of multiple staging.

In this subsection we discuss the manner in which the previous derivations give the performance of agglomerator sections in series. In the next section, an alternative or complementary approach is described in which feedback of particles is used to improve efficiency. Staging, whether by means of series sections, feedback, or both, is a trade-off with loading and ultimately, overall systems considerations will dictate which combination of equipment and loading should be used.

1. Series Staging

A series system of s stages is shown in Fig. (III.5). Each stage consists basically of charging wires and a drift space for mixing and agglomeration, as sketched in Fig. I.1. Parameters for each stage are summarized with the figure. We will assume that each charging section renews the charge/particle to the same value as that achieved at the inlet to Stage 1. Thus, $q_1(0)$ is the same for each stage, but in general, the loading of n_1 at the stage inlets varies, hence each stage has its associated loading parameter and characteristic decay length, ℓ^*. For the i'th stage, we have [from Eq. (III.22)],

$$\frac{n_1^i}{n_1^{i-1}} = \left\{ \frac{1}{\eta_i} + \left[1 + \frac{1}{\eta_i}\right] e^{\eta_i \ell_i / \ell^*} \right\}^{-1} \qquad \text{(III.30)}$$

$$i = 1,2, \ldots\ldots \quad s.$$

and hence the removal of particulate for the system as a whole is

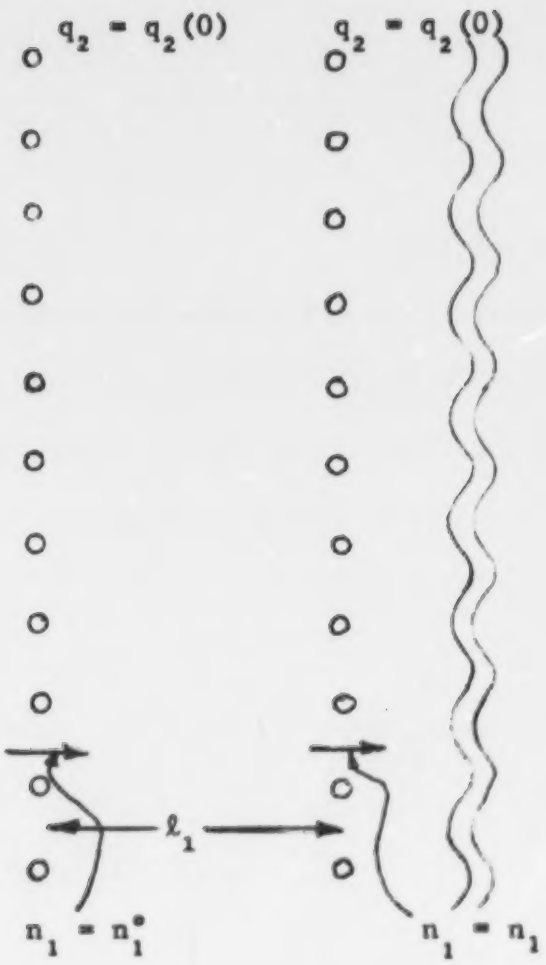

Stage 1

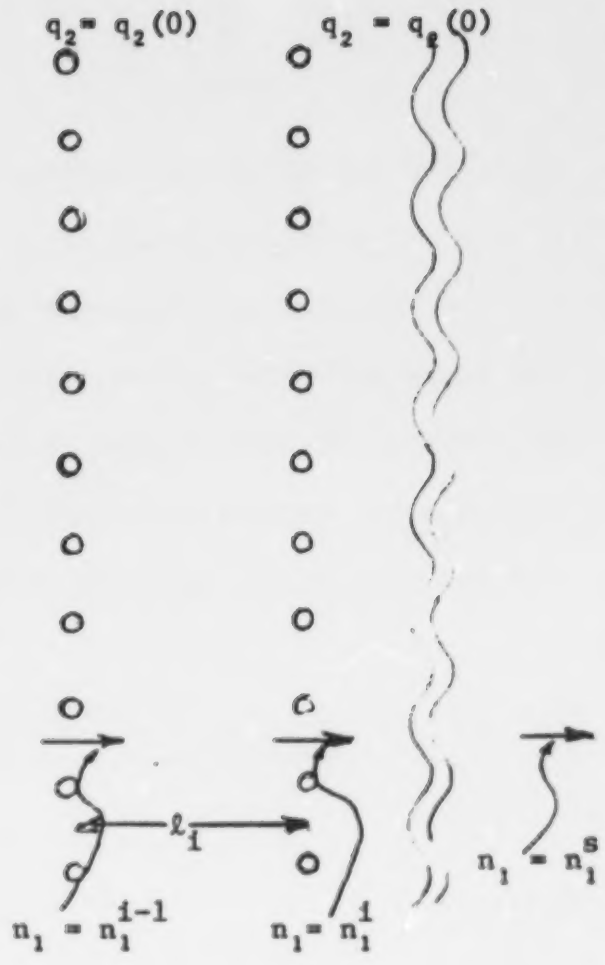

Stage i

n_1^i = number density of particles n_1 leaving i'th stage

ℓ_i = agglomeration length of i'th stage

$q_2(0)$ = saturation charge/particle of q_2 family at charging section

η_i = $[q_2(0)n_2/q_1 n_1^{i-1} - 1]$

ℓ_i^* = $6\pi\mu a_1 \varepsilon_o U/q_1^2 n_1^{i-1}$

Fig. III-5 Series system of agglomerators and associated definition of stage parameters

$$\frac{n_1^s}{n_1^\circ} = \prod_{i=1}^{s} \left(\frac{n^i}{n^{i-1}} \right) \qquad \text{(III.31)}$$

where the parameters are defined with Fig. III 5.

2. Particle Feedback for Improved Efficiency

Another way of increasing the efficiency of the system is to use the large and quite valuable particles more than once in a given section. This is accomplished if some of the particles at the outlet of the total agglomerator section (perhaps itself consisting of a series of stages) are fed back to the input as illustrated in Fig. III.6.

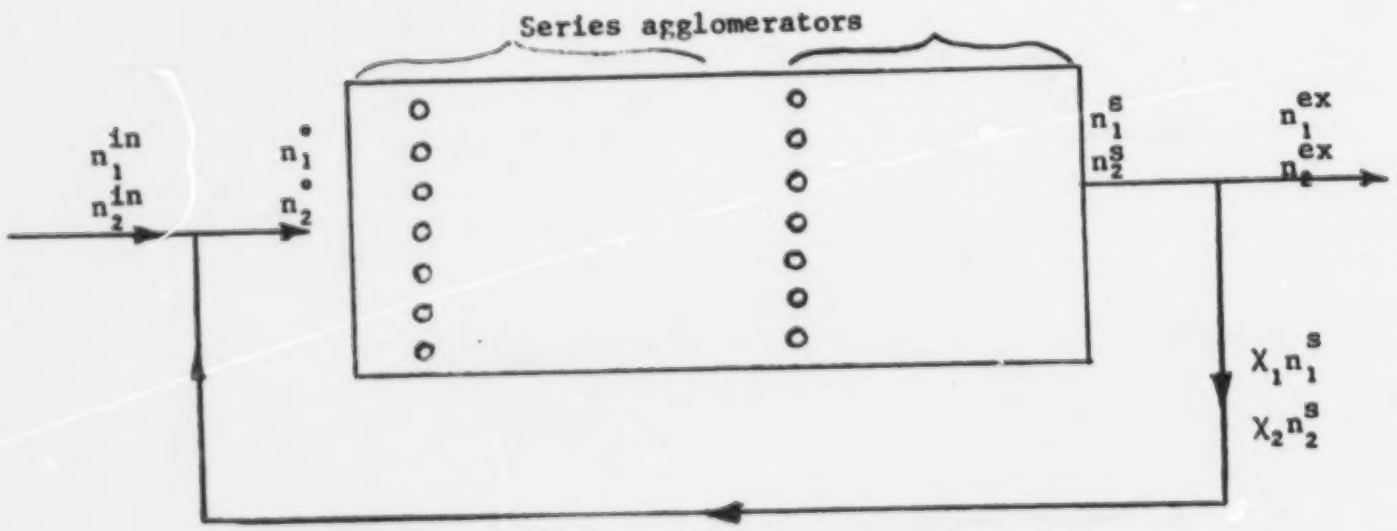

Fig. III.6 Feedback system around a total agglomerator consisting of one or more stages

---

The feedback is illustrated for the two-family system, but the general approach which is outlined could be equally well applied, with some complication, to a larger number of families.

The relation between input and output number densities n_j^{in} and n_j^{out} is required. A fraction $\chi_j < 1$ of the $j^{'th}$ spectrum is separated and fed back to the inlet of the agglomerator ($0 < \chi_j < 1$). The general problem is complex, because the relationship between n_j and n_j^s for a given family depends on the resident number densities of other families. However, in our picture of the agglomeration process, the number density of the largest family of particles is uncoupled from those below and we have the feedback relations

$$n_2^s = n_2^\circ \tag{III.32}$$

$$n_2^{ex} = n_2^s - \chi_2 n_2^s \tag{III.33}$$

$$n_2^\circ = n_2^{in} + \chi_2 n_2^s \tag{III.34}$$

from which it follows that $n_2^{ex} = n_2^{in}$, but more important, that

$$n_2^s = n_2^\circ = \frac{n_2^{in}}{1 - \chi_2} \tag{III.35}$$

Thus, the large particle number density in the agglomerator is enhanced.

Now, we can define a "gain" $G > 1$ for the agglomerator section defined, such that

$$n_1^s = n_1^\circ / G_1 \tag{III.36}$$

where, from Eqs. (III.22) and (III.31),

$$G_1^{-1} = \prod_{i=1}^{s} \left\{ \frac{1}{\eta_i} + \left[1 + \frac{1}{\eta_i}\right] e^{\eta_1 \ell_i / \ell^*} \right\}^{-1} \tag{III.37}$$

and the effect of feeding back the large particles is to increase η and

hence increase G_1 as computed from Eq. (III.37). But, in addition, a fraction χ_1 of the small particles is fed back; this fraction might be most conveniently selected as equal to that for the large particles. In any case, feedback relations for the small particles are, in addition to Eq. (III.36),

$$n_1^{ex} = n_1^s - \chi_1 n_1^s \tag{III.38}$$

$$n_1^* = n_1^{in} + \chi_1 n_1^s \tag{III.39}$$

and it follows that the output number density is related to the input density be

$$\frac{n_1^{ex}}{n_1^{in}} = \frac{(1 - \chi_1)}{(G_1 - \chi_1)} \tag{III.40}$$

Thus, the feedback accomplishes an improvement in the efficiency of particle agglomeration by subjecting the small particles to more than one pass through the agglomerator, as reflected by Eq. (III.40), and also improving the effect of the agglomerator in attenuating the small particles because of the residence of a larger number of particles [Eq. (III.37) with η computed using $n_2 = n_2^s$ from Eq. (III.35)].

F. Numerical Studies and Examples

To estimate the effectiveness of such a device in an industrial application, we will examine a one-stage device which operates on the fly ash produced by burning pulverized coal in an electric power station. The mass distribution in such a flow is given in Fig. (III-7a). Notice that all sizes from less than 1μ to greater than 100μ are represented. In order to transform the distribution to make it compatible with our two-particle analysis, we will make the following, somewhat arbitrary, identification. The

particulate mass distributed between a = 0 and a = 1 will be redefined as the small particle density m_1 centered at $a_1 = 0.5$. The remaining mass, which in this case represents 99% of the total, will be defined as the large particle mass density with an effective radius of 10μ. This redefined distribution is shown below in Fig. III.7b:

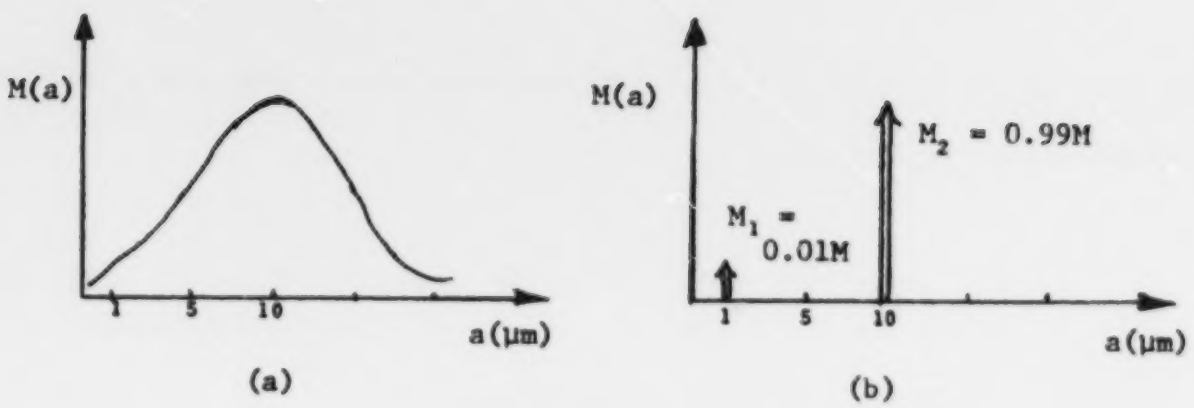

Figure III.7 Mass distribution for fly ash from pulverized coal; M is the mass concentration, i.e., the mass of particulate per unit volume of gas

---

For a typical total particulate loading of $M = 7 \times 10^{-3}$ kg/m^3, that part attributed to the small particles will be $M = 7 \times 10^{-5}$ kg/m^3. The loading factor in this case will be given by

$$\eta = \left(\frac{a_1}{a_2}\ \frac{V_2}{V_1} - 1\right) = \left(\frac{a_1}{a_2}\ \frac{M_2}{M_1} - 1\right) = \left(\frac{5 \times 10^{-7}}{10^{-5}}\ \frac{7 \times 10^{-3}}{7 \times 10^{-5}} - 1\right) = 4 \qquad \text{(III.41)}$$

The spacing factor, α_1, can be determined from the following relation

$$n_1 \triangleq \frac{1}{(\alpha_1 a_1)^3} = \frac{M_1}{m_1} \rightarrow \alpha_1^3 = \frac{m_1}{M_1}\frac{1}{a_1^3} \qquad \text{(III.42)}$$

$$\alpha_1 = \left(\frac{1.25 \times 10^{-16} \text{ kg/part}}{7 \times 10^{-5} \text{ kg/m}^3}\right)^{1/3} \frac{1}{(5 \times 10^{-7} \text{ m})} = \frac{(0.78 \times 10^{-11})^{1/3}}{5 \times 10^{-7}} = 242 \; . \qquad \text{(III.43)}$$

Finally, the decay constant is now seen to be:

$$\ell^* = \frac{\alpha_1^3 \mu U}{24 \pi \varepsilon_o E_o^2} = \frac{(242)^3 (5 \times 10^{-5}) (5)}{(24)(\pi)(8.85 \times 10^{-12})(10^6)^2} \cong 5.3 \text{ m} \qquad \text{(III.44)}$$

Using the results of § III.d-2, we can determine the density and charge distributions down the channel:

$$\frac{n_1(x)}{n_1(0)} = \{ -0.25 + 1.25 \, e^{0.75x} \}^{-1} \cong 0.8 \, e^{-0.75x} \qquad \text{(III.45)}$$

$$\frac{q_1(x)}{q_1(0)} = e^{0.75x} \{ -0.25 + 1.25 \, e^{0.75x} \}^{-1} \cong 0.8 \qquad \text{(III.46)}$$

To achieve a removal efficiency of 99.9% for the small particulate, i.e., to have $\frac{n_1(x)}{n_1(0)} = .001$, we must make the agglomeration region at least 8.9m in length.

The above conclusion assumes that we are operating just one stage. Suppose that we cascade two of them, each a meter in length. The output small particle concentration is given by Eqs. (III.30-31) for s = 2 and $\ell = \ell_2 = 1$

$$\therefore \frac{n_1^2}{n_1^o} = \frac{n_1^1}{n_1^o}\frac{n_1^2}{n_1^1} \cong (0.8 \, e^{-0.75})(0.92 \, e^{-0.87}) = 0.145 \qquad \text{(III.47)}$$

Notice that, in cases like this where $\eta > 1$, the effect of adding more stages, rather than just extending the length of the first, is not particularly significant.

To enable us to meet specifications with a shorter length of a single-stage system, we will feed back part of the large particles exiting to the input. Thus, let $\chi_2 = 0.9$ and $\chi_1 = 0$. From § III.E,

$$n_2^s = n_2^\circ = \frac{n_2^{in}}{1 - \chi_2} = 10\, n_2^{in} .$$

Thus,

$$C_1 \tilde{=} e^{\eta_i \ell_i / \ell_i^*} = e^{9.25 \ell_i} \qquad \text{(III.48)}$$

To meet the same efficiency requirement as before, $n_1(x)/n_1(0) = 0.001$, the length of the agglomeration region must be at least 0.72 m. This is a significant reduction in the required length of the system.

In passing, it should be pointed out that, even though we have increased the large particle concentration by a factor of ten, they are still fairly well dispersed. Feedback has reduced α_2 from 52 to 24. Any additional feedback would clearly call into question our assumption that the larger particles behave as independent entities.

IV. Experimental Studies

A. Experimental Objectives

Experiments reported here are aimed at demonstrating the existence of electrically-induced agglomeration of small particles on large ones. Ideally, the charging scheme results in essentially bipolar concentrations of all sizes of particulate, hence the desired agglomeration must be demonstrated in regions of no macroscopic electric field. As pointed out in § II.A, electrically-induced agglomeration at walls is well documented and in practical use. A major consideration in interpreting experimental results is therefore distinguishing between agglomeration at walls and in the "bulk".

B. Preliminary Observations

The choice of a particle system is made in the face of many considerations. If possible, the particles should be representative of those found in practical application, but also, existence of two distinguishable particle sizes at the input is necessary.

The first tests used the flow system shown in Fig. IV.1. The choice for the large particulate was sodium bicarbonate, with a radius of about 100μ , and for the small was fly ash, with radius of about 1μ. Since the large particles were crystals and the small ones amorphous, any significant coagulation of the latter on the former could readily be detected. Sampling of the flow was accomplished with a small electrostatic precipitator at the end of the channel, where part of the collection surface was occupied by a tin oxide coated slide. Tests with dc and 60 Hz. and 400 Hz. ac failed to leave any agglomeration proof on the slide. In addition, the optical character of the flow did not change when the corona was turned one. That

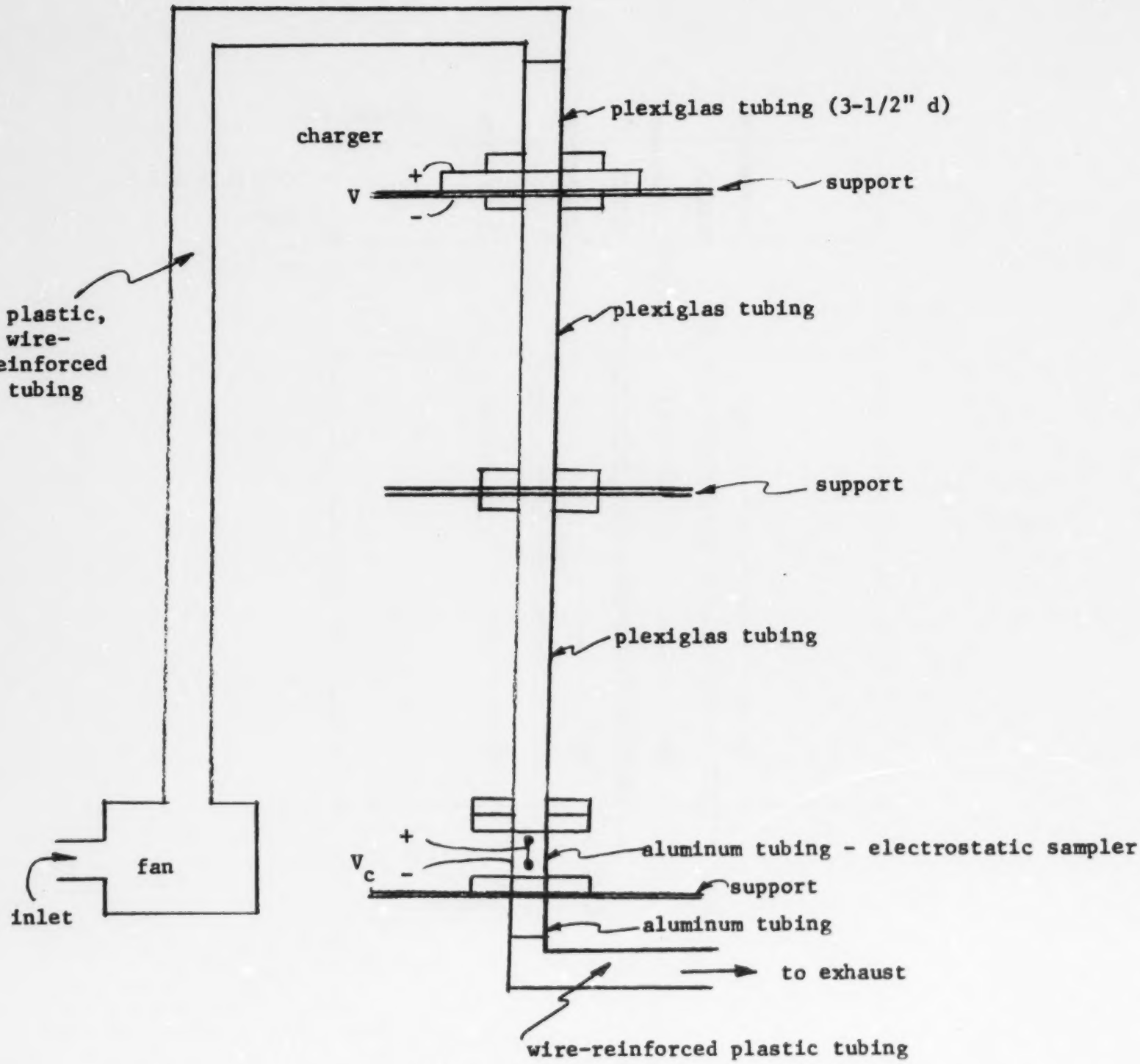

Figure IV-1a Flow system used for study of interactions between cold particles

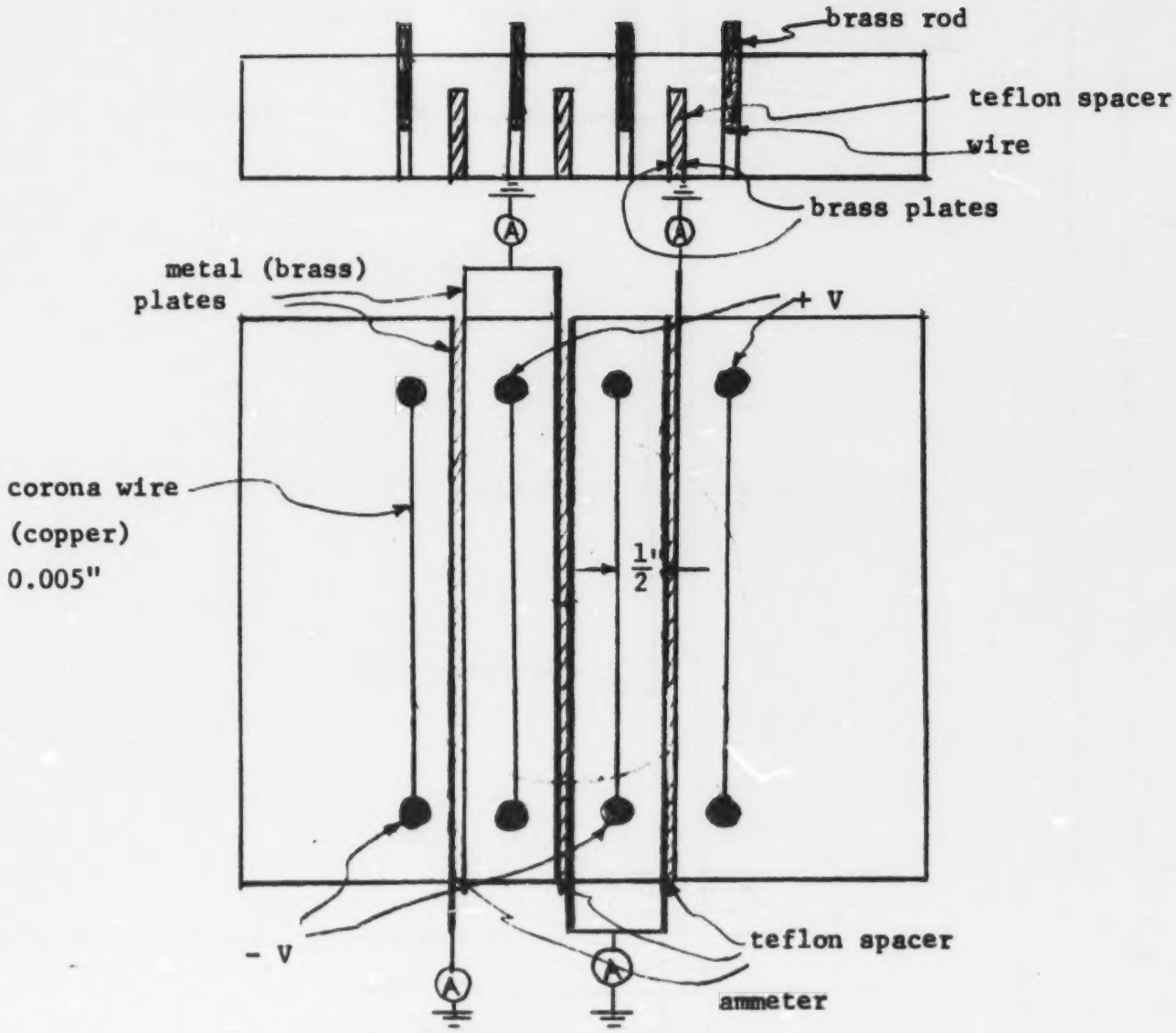

Figure IV-1b Charger configuration consisting of parallel corona discharges of alternate polarity

is, the turpidity of the flow did not seem to be significantly altered.

In the course of these experiments, it was noticed that both the fly ash and the sodium bicarbonate exhibited very little tendency to stay together, once they were placed in contact with other particulate. This lack of adhesion did not bode well for any sort of agglomerative process. A search was then made for another type of particulate which possessed good adhesive qualities and could be readily dispersed. The selection finally came to oil smoke. Besides having the other two attributes, these fumes closely resembled some of the pollutants that were actually of concern to industry, and could be produced in a manner that closely resembled an industrial operation.

The brief test conducted on agglomeration under cold-flow conditions should not be construed to indicate that agglomeration cannot be achieved in particle systems of the fly-ash type. Oil ash was selected as an attractive alternative because then the issues of agglomeration and adhesion could be more clearly separated. To simulate actual particle adhesion properly, hot-loop tests with fly ash should be conducted, rather than the cold-flow tests used in these preliminary experiments.

C. Oil-fired Experiment: Test Facility

The experimental layout of the oil-fired system is given in Fig. IV.2. A home oil burner, with continuous ignition from a spark gap, was used to burn a No. 2 Diesel fuel. The flame was passed through an array of cast iron pipes, the first section of which was cooled with a water jacket consisting of many turns of copper tubing. The array served to stretch out the flame and remove much of the excess heat from the gas flow before it reached the next section, constructed of sheet metal ducting. After a five-

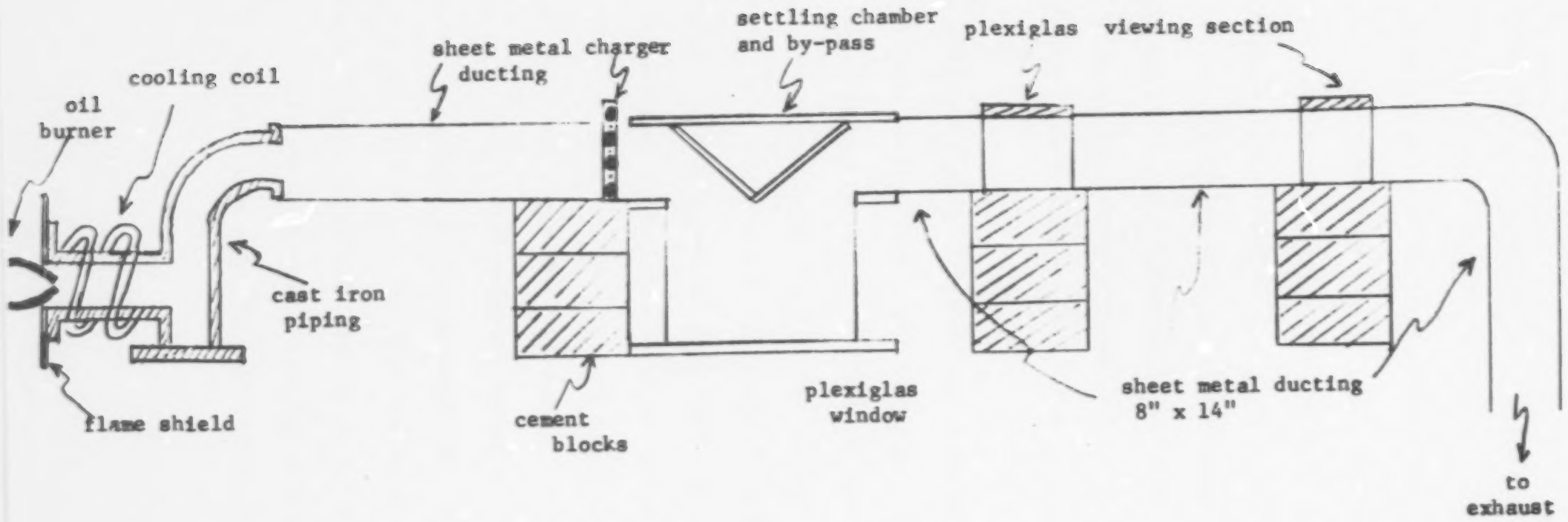

Figure IV-2 Oil-fired agglomeration test facility

foot length was placed the charger. As seen in Fig. IV.3, this consisted of half-inch bars and thin wire, alternately spaced horizontally across the flow. The flow could next be directed either straight through, or diverted through a settling chamber three feet in diameter. The gas was then drawn through two other five-foot sections of ducting before finally reaching the exhaust channel.

D. Oil-fired Experiment: General Observations

In these experiments, the burner was adjusted with its air intake significantly restricted, so that a dark black smoke was produced. A typical photomicrograph of a tin-oxide-coated slide used in a sampling electrostatic precipitator placed at the end of the channel is shown in Fig. IV.4. The particulate illustrated is with the charger off and is typically in the size range of one micron.

During the first series of tests, the bars of the charger section were grounded, and alternate wires were set at positive and negative high voltage. These were adjusted so that the total amount of positive corona current equaled that of the negative. A dramatic change in the character of the dispersion was easily observed with the application of the charging voltages. The flow downstream rapidly turned from a dense smoke into large dispersed flakes; this change, from the dense smoke with the corona off to the dispersed large flakes with the corona on, occurred in less than one second. Photographs of the downstream flow taken using transmitted light across the approximately one-foot flow width are shown in Fig. IV.5. A single stroboscopic flash was used, and channel side walls were not present. (By using a negative pressure at the outlet, it was possible to observe processes without an intervening wall at tests points along the length.)

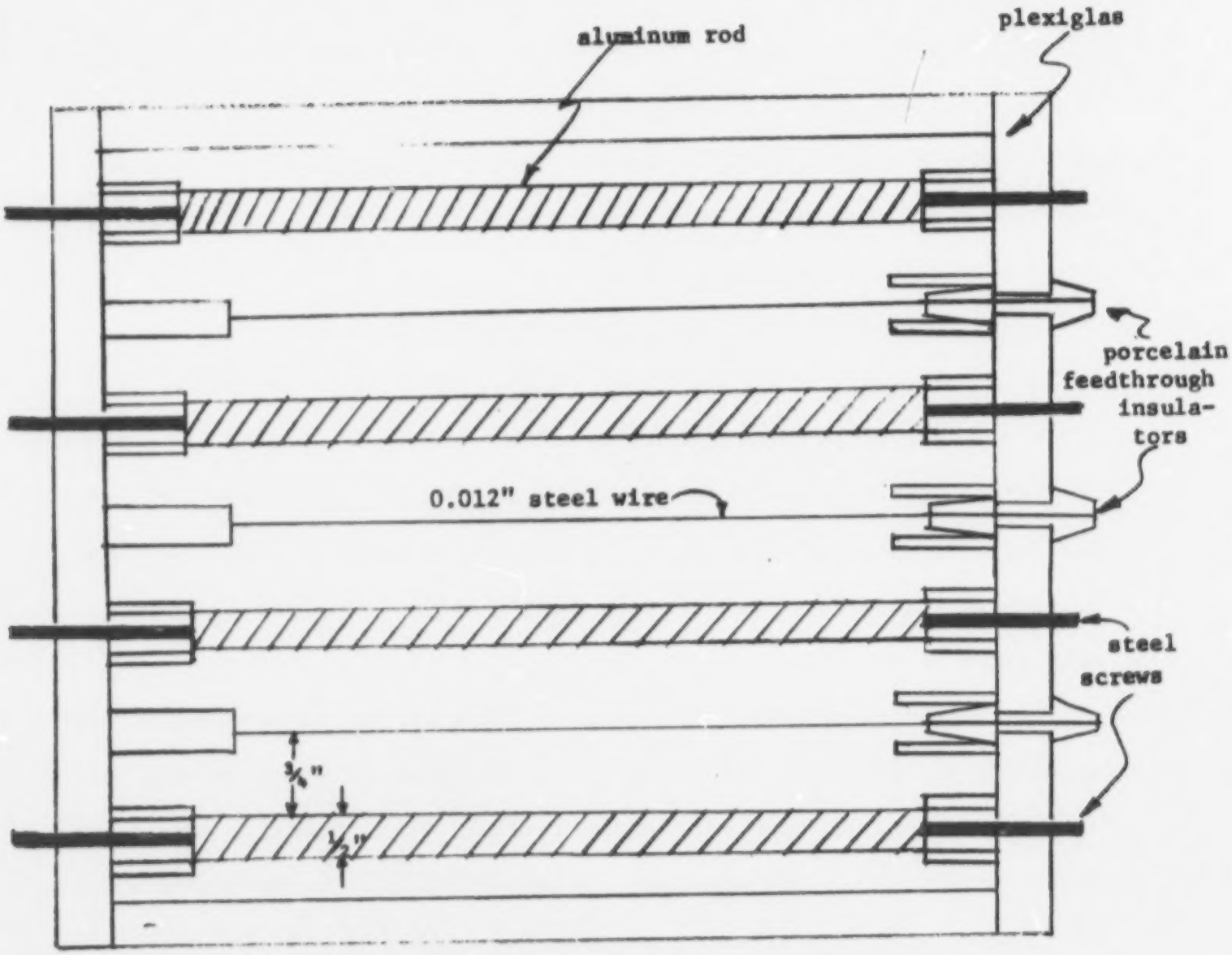

Figure IV -3 Charger section used in oil-fired experiments

(a)

NOT REPRODUCIBLE

(b)

Figure IV-4 Photomicrographs of samples of electrostatically precipitated oil smoke: (a) X 100 (b) X 1,000

(a)

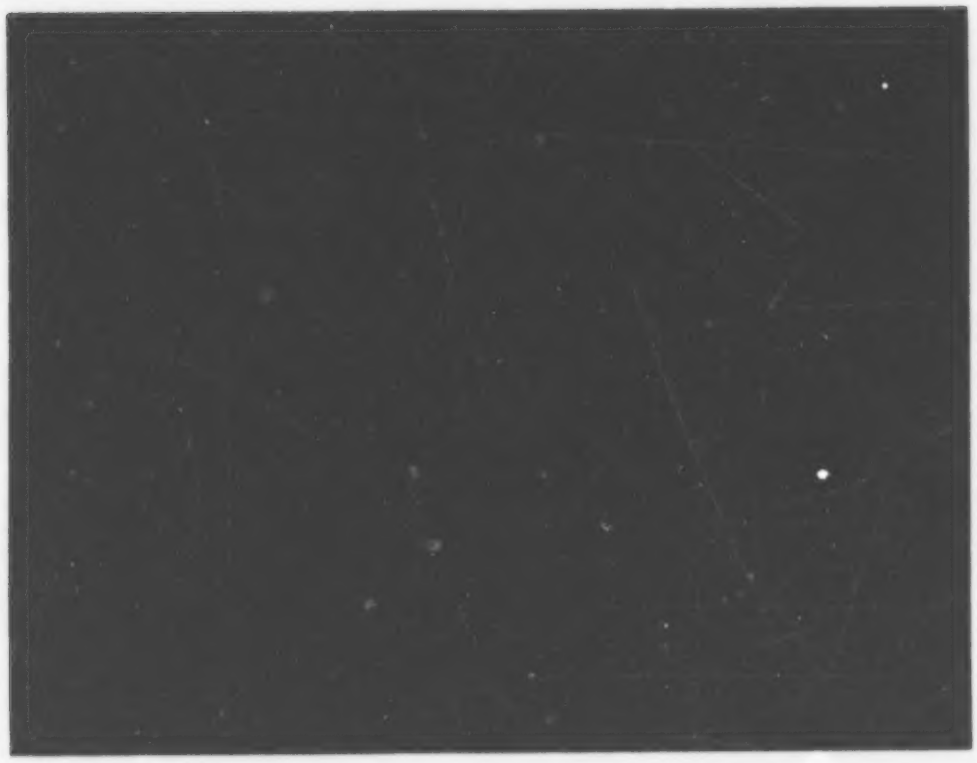

NOT REPRODUCIBLE

(b)

Figure IV-5 Photographs of flow just in front of exhaust inlet.
(a) Without corona (b) With corona

Seemingly paradoxical was the further finding that this electrically-induced agglomeration was, if anything, enhanced if all the electrode wires were placed at the same positive (say) high potential. That the electrically-induced agglomeration was obtained with unipolar corona charging seemed to contradict the postulate that agglomeration is caused by the attraction of oppositely charged particles through their micro fields. However, examination of the charging process made it clear that the charging section was serving two essential purposes, even with only one polarity of excitation. It provided not only bipolar charging of the particulate, but also produced the families of large sized particles requisite to the desired agglomeration process.

As described in the next section, the charging section, as operated, functions as a form of wall-type agglomerator. An important part of the electrically-induced agglomeration so evident in the outlet stream (Fig. IV.5) occurs in the charging section. Thus, it is crucial that tests for the desired bulk agglomeration distinguish between the agglomeration in the charging section and bulk agglomeration in the region of no net electric field following the charging section.

E. Pre-agglomeration at the Charging Section Surfaces

In this section of the report, we discuss the charging process itself. We present experimental evidence that the output of the charging section is in fact composed of bipolar charged particles in two disparate size ranges. The details of this charging dynamics are of considerable interest in their own right, and can only be indicated in a tentative way here. The objective of the tests reported here is evidence for the bulk agglomeration. Hence, charging section dynamics are pursued only to the extent of substantiating

the bipolar polydisperse output and roughly indicating the underlying mechanism. Then, in §F, the evidence for bulk agglomeration is presented.

That the charging section behaves as a wall-type aggomerator is based in part on direct observation of the particles being collected and removed at the charging bars and wires. The flow is observed under operating conditions with a minimum of obstruction by simply providing a break in the duct. As mentioned earlier, the negative pressure at the outlet provided sufficient suction that the particulate flow remained confined in passing from upstream to downstream sections of the channel. A complete cross section of the flow is then observed without obstruction due to walls either in front of or behind the flow. In the pictures shown in Fig. IV.6, the charging electrodes and wires are viewed through such a gap. These typify slow-motion films made to determine the nature of the charging process.

The strong influence of the electric field and associated charged particles can be seen in the figure, which shows the flow with and without an applied voltage. Without voltage, the smoke provides a ready visualization of stream lines around the bars and wires, with a boundary layer in the neighborhood of the former evident. With a corona current, the region surrounding bars and wires is filled with smoke in a homogeneous way. The flow in the charging section neighborhood becomes "fuzzy" and there is little visual evidence of the boundary layer around the bars.

Close observation of the bars shows them to be the site of particle collection and dispersal. Several features of the apparent processes occurring in this region relate to our objectives.

The electric field produces a type of "turbulence" in the neighborhood of the bars and wires and in the intervening gaps [15]. There are

(a)

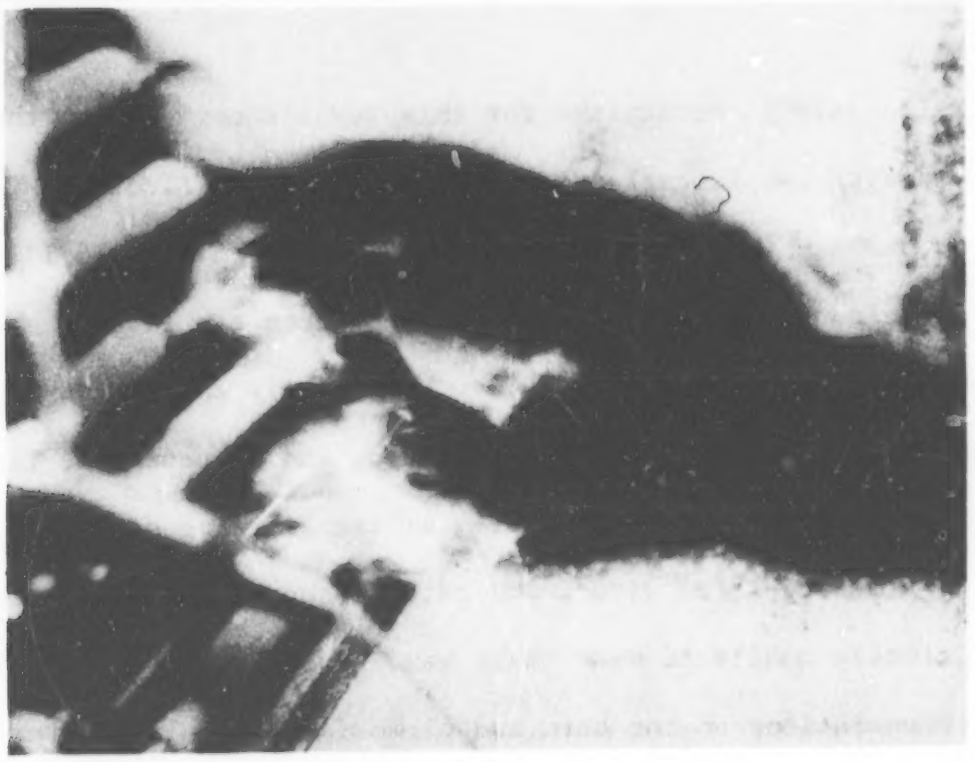

NOT REPRODUCIBLE

(b)

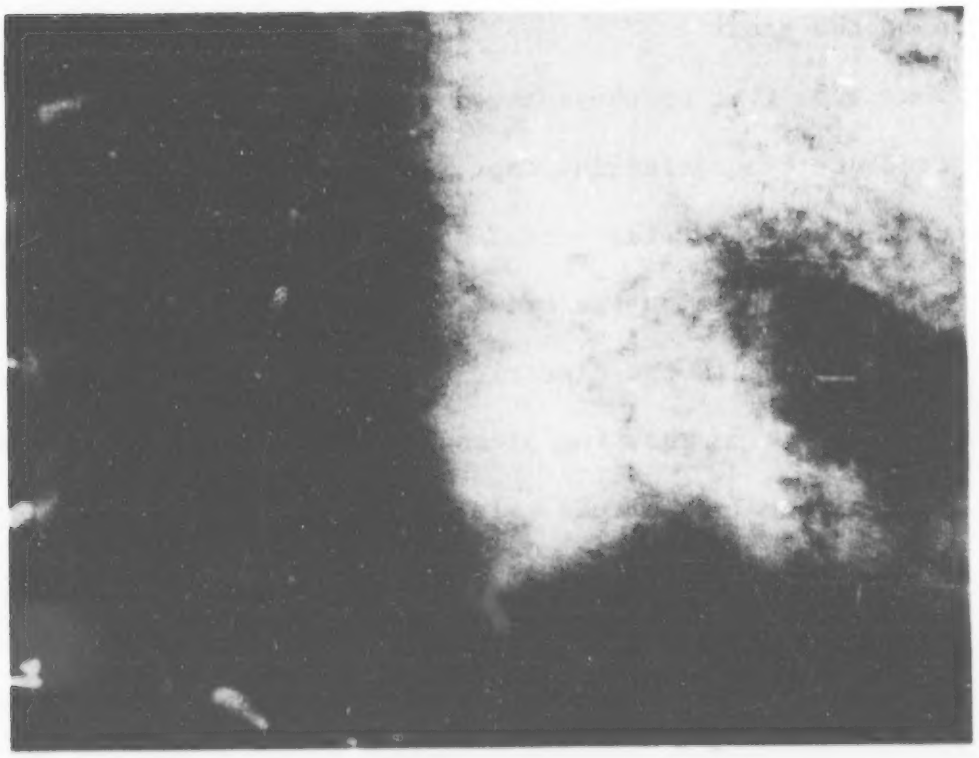

Figure IV-6 Charging Section

(a) Without corona (b) With corona

several available mechanisms for this turbulence. First, the ion flow from wire to bar is certainly accompanied by an "Electric Wind" which can be on the same order as the flow velocity of the gas [16,17]. Second, the space charge in the vicinity of the wires can lead to a fine-scale turbulence from instability [18]. Here, it is the region adjacent to the wire that is most likely to be affected, and of course it is that region which is most significant in terms of transferring particles from the gas to the electrodes, or wires. Third, the charged particles themselves are sufficiently mobile to make their way across the flow, as is evident from the accumulations on the bars and wires (an accumulation that does not occur in the absence of a corona current). These particles produce a drag on the surrounding air which can contribute to the apparent fine-scale motion of the gas.

That the first of these three mechanisms is influential can be lent some credence by considering that, under conditions of space-charge-limited conduction at the corona source, the electric field makes available a pressure rise on the order of $1/2\ \varepsilon_o E^2$ where ε_o = permittivity of free space, and E is the electric field intensity in volts per meter. Hence, if we assume that the pressure rise goes into acceleration of the fluid, an order-of-magnitude calculation is given by equating the electric pressure and $1/2\ \rho v^2$ (Bernoulli dynamic pressure)

$$v = \sqrt{\frac{\varepsilon E^2}{\rho}} \qquad \text{(IV.1)}$$

Typical numbers give

$$v = \sqrt{\frac{(8.85 \times 10^{-12})(3 \times 10^6)^2}{1}} \approx 10 \text{ m/sec} \qquad \text{(IV.2)}$$

or a velocity well above that used in the experiments. Hence, it is plausible that ion-drag pumping contributes appreciably to mixing across the gas flow between bars and wires.

That the charged smoke particles can make their way across the gap, even if they are not carried by the "corona wind", is made plausible by the following calculation. Assume that the particle charging mechanism is governed by an impact model. The time constant involved in such a model is

$$\tau = \frac{4\varepsilon_o}{b_i \rho_i} \tag{IV.3}$$

where b_i is the ion mobility and ρ_i is the ion charge density. But the corona current is given by

$$I = \rho_i b_i E A. \tag{IV.4}$$

Thus,

$$\tau = \frac{4\varepsilon_o E A}{I} \tag{IV.5}$$

$$\tau = \frac{4(8.8 \times 10^{-12})(10^6)(2.6 \times 10^{-2})}{(2.5 \times 10^{-4})} \cong 3 \times 10^{-3} \text{ seconds} \tag{IV.6}$$

Since the above time is short compared with the time required for a particle to pass through the charging section (about 10^{-2} sec), the particulate is taken to be charged to its saturation value and its subsequent transverse motion to be governed by the electric force balanced by Stokes' drag. Thus,

$$q_s = 12\ \pi\varepsilon_o E a^2 \tag{IV.7}$$

and

$$v_t = \frac{q_s E}{6\pi\mu a} = \frac{2\varepsilon_o E\ a}{\mu} \tag{IV.8}$$

For 1μ particles:

$$v_t = \frac{(2)(8.8 \times 10^{-12})(10^6)^2(10^{-6})}{2 \times 10^{-5}} = 1 \text{ m/sec.} \tag{IV.9}$$

This is on the same order as the longitudinal gas flow velocity. Thus, since the interaction zone is about as wide as it is long, a sizeable percentage of the incoming particles should be able to traverse the inter-electrode distance and be plated on the bars before being swept out of the zone.

Our picture of the charging process is as follows. Smoke particles in the size range of 1μ (and with few greater than 10μ) enter the charging section with essentially charge neutrality. That random charging in the combustion process and prior flow is negligible is confirmed by the insignificant interaction of the particles with downstream electrified electrodes with the corona current off. The corona current is responsible for charging of these small particles by ion impact. So, with the corona wire positive, the smoke particles are charged positively.

The time for this process to reach saturation is on the order of 10^{-3} seconds while the transit time through the charging section is of the order 10^{-2} seconds, even if there are no effects on the flow by the electric field. Hence, there is time for the particles to be charged. These positively charged small particles are drawn to the charging bars by the electric field (and also by the corona wind effects discussed earlier). On reaching the bars, they first adhere and almost instantaneously reverse their charge polarity because of charge induction (the electrical relaxation time of the particles is less than 10^{-11} seconds). The combination of wind friction from the gas flow and the electrical force, which now tends to draw the particle away from the electrode surface, eventually results in the material leaving the electrode, but this time in the form of agglomerates. What has been described here is, of course, the wall agglomeration referred to in § II.A.

From observation of the flow just downstream from the charging electrodes, it is evident that only a fraction of the particles have gone through the process of charge reversal and wall agglomeration. High-voltage electrodes placed in the flow interact strongly with both the large particles and the smoke, indicating that both are charged. Both the wires and the bars show particle accumulations, so that some of the particles make their way back to the corona wires. They then act in a manner similar to that of the bars in providing for agglomeration. The charging section therefore provides large particles of both polarities, but not in equal numbers. Once the flow has left the charging section, there is no evidence that the particles taken together have a net charge. In the settling chamber experiments of the next section, no radial drift of particles from the fluid volume is observed, as would indicate the existence of an appreciable macroscopic field due to space charge.

F. Volume Agglomeration in the Drift Zone

It is a qualitative observation that, with the application of the charging voltage, the flow appears to become clearer of the small particles at intervals down the channel. Also, the size of the large agglomerates seems to increase. This is, of course, the behavior expected from an agglomeration process in the volume of the flow following the charging section. Except for the purpose of sampling the flow, the mixture of large and small charged particles is essentially in a region of charge neutrality within the duct and in the settling chamber to be described shortly. It is the lack of an ambient electric field that makes the wall-type agglomeration unlikely in the drift zone. Nevertheless, the objective of the following tests is to be sure that agglomeration subsequent to that

in the charging section takes place in the volume, and not at the walls.

A crude verification of the observations above is given in Fig. IV.7. The flow is sampled at intervals with pieces of white gauze inserted briefly transverse to the flow. Without corona, the gauze turns a light shade of grey. With corona, it turns black with a coating which, on closer examination, proves to be large black flakes. The effect of the charging on the size of the particles is obvious. But also, notice that the darkening of the first two samples is about the same, while that of the third, placed furthest downstream, is greater. This is only a crude indication of the desired performance.

Photographs such as those illustrated by Fig. IV.5 lend further support to the agglomeration occurring in part between the charging section and the channel outlet. Photographs taken using stroboscopic light just downstream from the charging section show some agglomeration, but the large particles are not nearly as evident as in Fig. IV.5, and the background of small particles is considerably greater.

There is the question of whether or not the observed agglomeration in the drift zone is due to the duct walls; as preliminary evidence, we noted that the distribution of large particles over the flow cross section is virtually uniform. If the agglomeration occurs at the walls, the density of large particles should be greatest near the walls. Further, upon removal of the charging section voltage, the large particles disappeared in the outlet flow in a time approximately equal to the transit time of the gas through the intervening duct. If agglomeration occurs at the walls, the large particles could continue to flake off the walls for some time after the charging section is turned off.

(a)

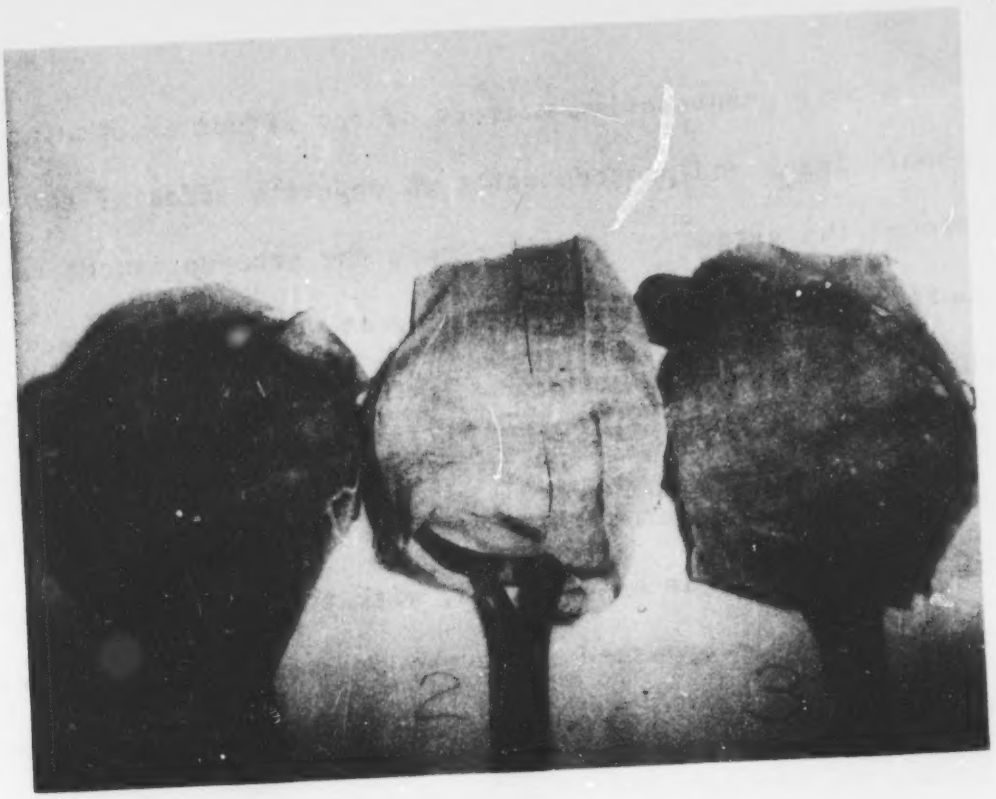

NOT REPRODUCIBLE

(b)

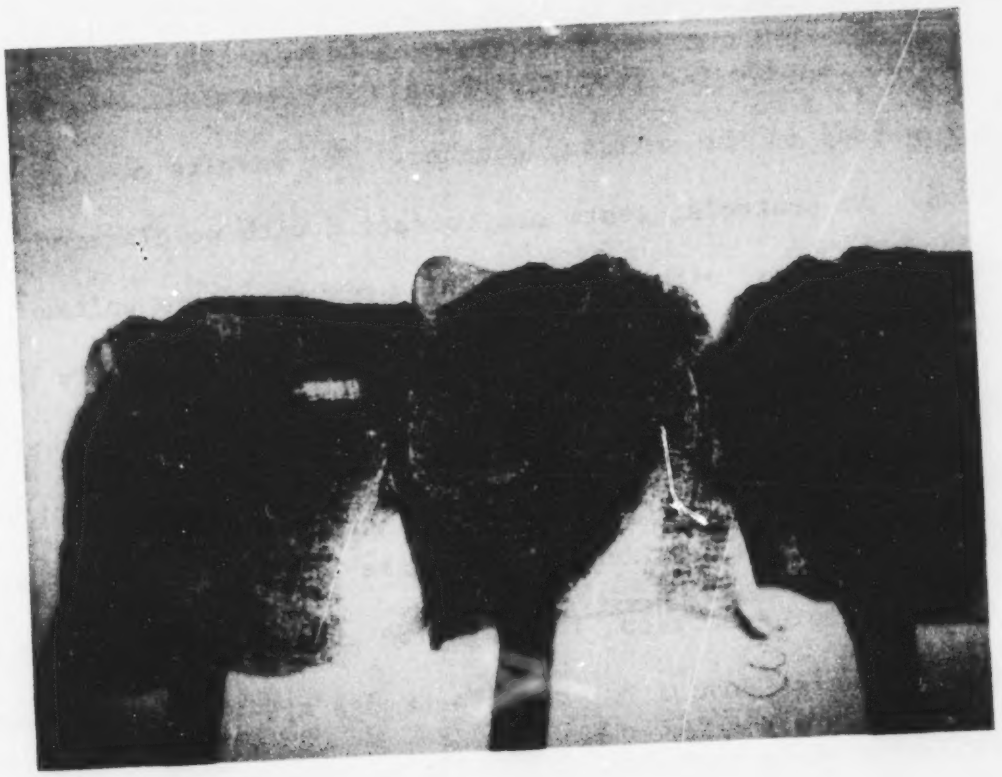

Figure IV-7 Gauze samples of flow, taken: 1) Just after charger; 2) Halfway down the channel; 3) Just in front of the exhaust. (a) Without corona (b) With corona

A more quantitative measure of the effect is obtained by placing a small laser and photodetector on opposite sides of the channel. Through the output of the detector, the attenuation of the light beam is monitored as the corona is switched on and off. This is one method by which the time-delay measurements are made.

The settling chamber shown in Fig. IV.2 is a convenient way to obtain improved control over the agglomeration process. To use the chamber, the steady-state flow is established, with the gas ducted through the chamber. Then the flow is bypassed above the chamber, which is closed off and therefore established in a quiescent condition. It is then possible to examine the particle behavior in the absence of aerodynamic effects, and obtain further evidence of (a) the bipolar charging of particles, and (b) desired volume of the agglomeration.

To observe the particle charging, electrodes covered by plexiglas are placed in the settling chamber. The results are typified by Fig. IV.8. As controls, tests are conducted with no electrode voltage and no corona voltage, with no corona but with electrode voltage, and with both corona excitation and sampling electrode voltage. Only the last gave appreciable collection. It is clear from these tests that the requisite bipolar charging of the large particles is present. Both electrodes collected particles, although as might be expected from the asymmetric excitation in the charging section, the negative particles are somewhat more numerous. The insulating covers for the electrodes are used to prevent the particles frmm rebounding upon striking. (It is observed that, if bare conducting electrodes are used in the settling chamber, very little of the particulate is collected on either electrode.)

(a)

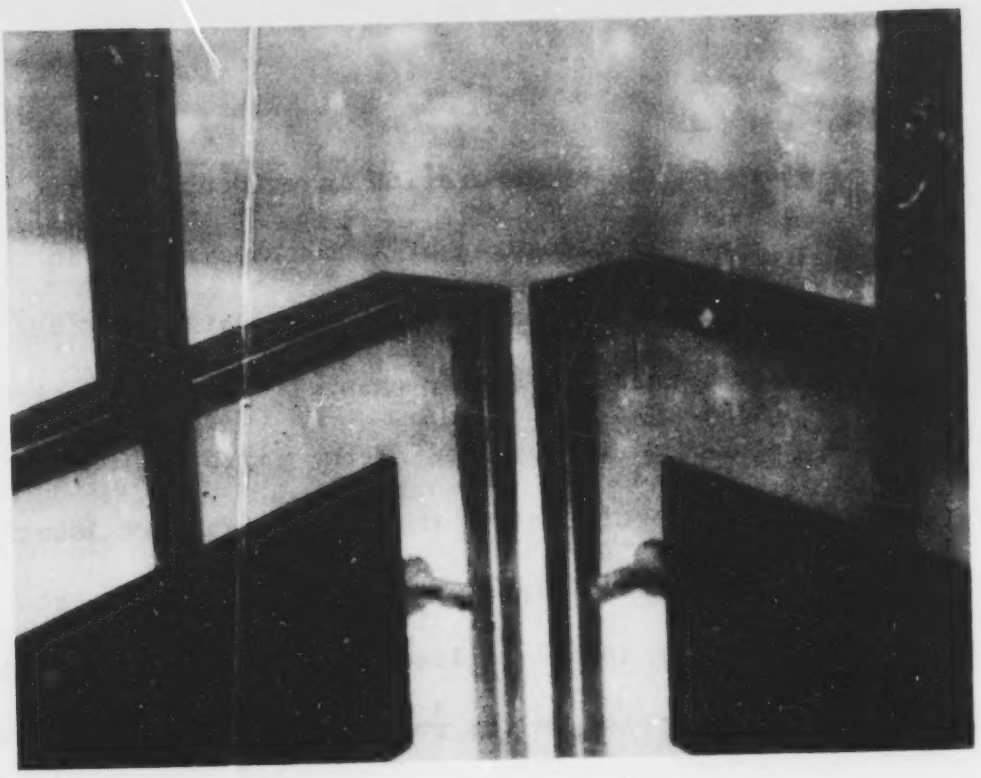

NOT REPRODUCIBLE

(b)

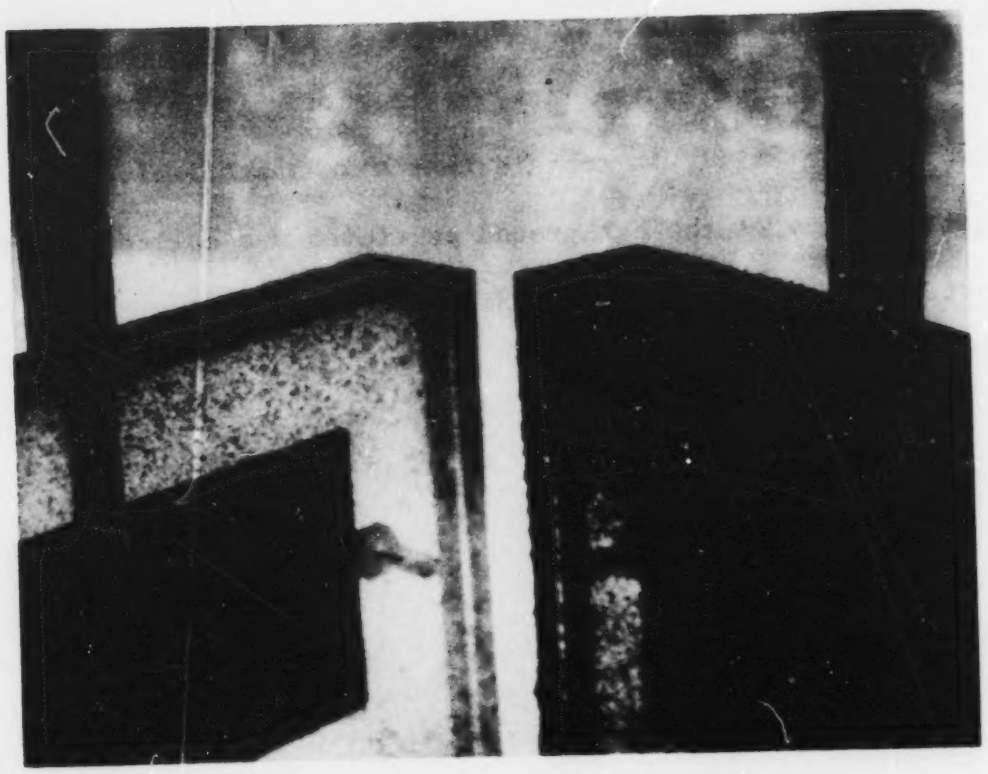

Figure IV-8 Sampling electrodes for:

(a) No corona; $V_L = -10$ Kv, $V_R = +10$ Kv

(b) Corona; $V_L = -10$ Kv, $V_R = +10$ Kv

L = left electrode R = right electrode

The history of the agglomeration is evidenced by the laser beam attenuation. A sample recording of beam transmission intensity is shown in Fig. IV.9. Without excitation of the charging section, the smoke particles age at a rate far slower than with the excitation. The attenuation with excitation is composed of two parts: a background part caused by the fine particles and the pulses that are identified with the passage across the beam of large particles. It is important to recognize that the chamber is initially filled homogeneously with smoke. The growth of large particles in the volume of the gas is obvious; note that the process occurs over the interval of tens of seconds. The transit time of the gas through the drift region of the duct is somewhat less than a second, so that only the initial part of the agglomeration process is exploited in the flow experiments. In terms of the theory developed in § III, it appears that η is appreciably greater than -1. That is, many of the background particles are collected before the large particles are fully discharged.

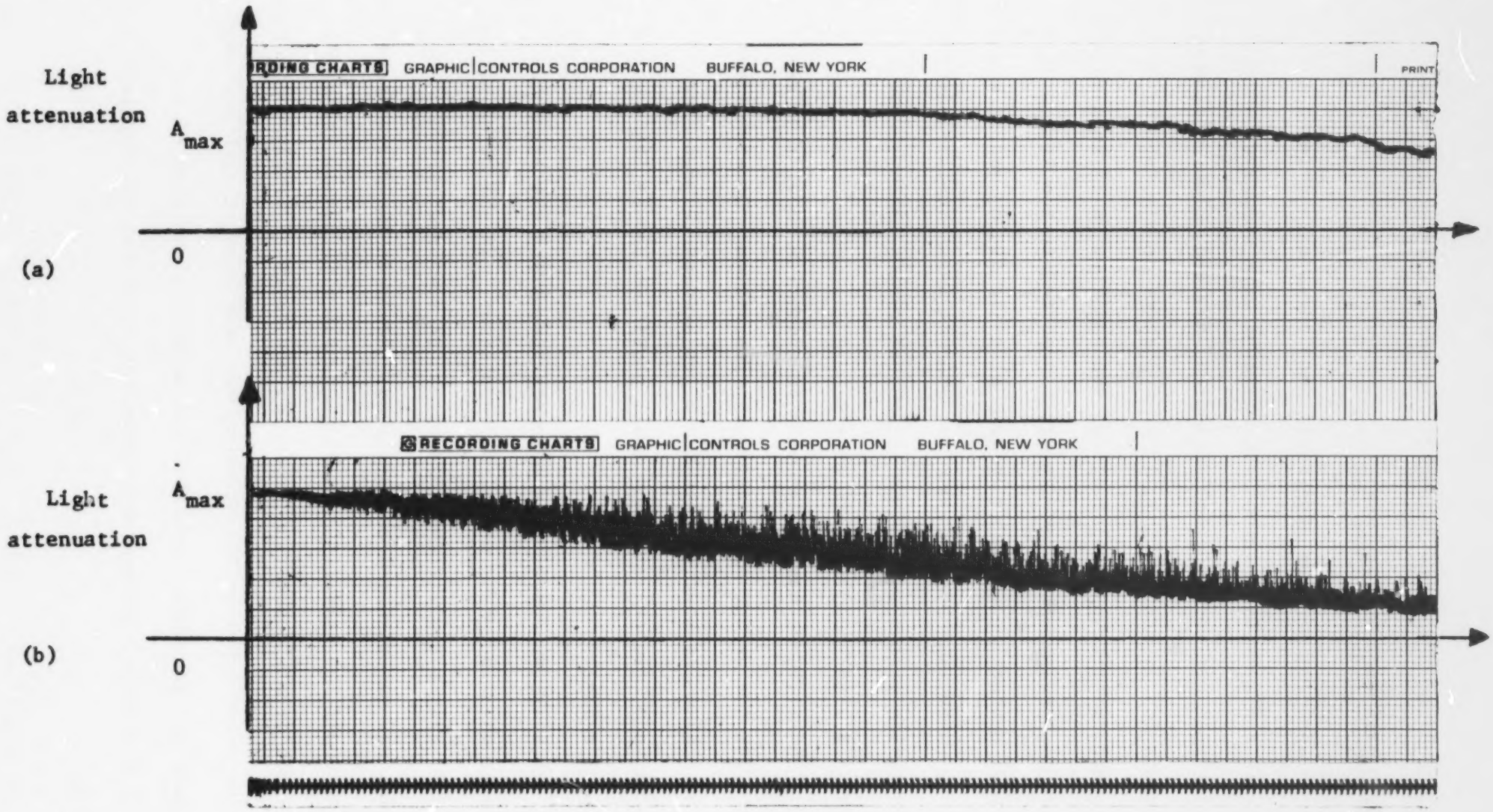

Figure IV-9 Settling chamber attenuation measurements

(a) Without corona (b) With corona

V. Summary Remarks and Conclusions

The contributions of this study fall into three categories.

First, in § II, we have summarized previous work described in the literature as relating to electrically-induced agglomeration. Because of implications for device scaling, it is important to distinguish between agglomeration processes that attend the application of an electric field. Most of the agglomeration processes reported in the literature in a practical context occur in an ambient electric field, and at walls. Nevertheless, there is some reference to apparent electrically-induced bulk agglomeration in the absence of an ambient field, although observations are of a highly speculative nature.

Second, in § III, we have advanced a quantitative model that can be the basis for the design of an agglomeration system. It seems clear from numerical examples that the agglomeration process through micro-field interactions between large and small particles can be implemented on a practical scale.

Third, in § IV, we describe experiments supporting the existence of volume agglomeration under practical conditions. In the brief period of this study, only a qualitative connection has been made between the systems model and experimental observations. It is in the direction of making this connection quantitative that the next step should be taken.

The choice of oil combustion products, and hence of highly conducting particles for these experimental studies, was made because such systems seemed to have the greatest likelihood for achieving adhesion of the agglomerated particles, through mechanisms not involving the particle charging itself.

Optimal design of electrostatic systems for efficiently removing fine particles from oil combustion products depends on making controlled experimental studies that advance confidence in the systems model. It seems clear from the work presented here that the volume agglomeration can be produced to an extent that warrants consideration in practical systems.

The experimental study using cold fly ash was set aside in favor of the hot-flow, oil-fired experiment, because of the limited time available. The use of volume agglomeration for solving problems connected with fly ash should be viewed as untried. Indeed, it is in the area of handling products of low-sulfur coal combustion that the agglomeration process offers a badly needed new departure. The agglomerator does not require the accumulation of particles having a net charge. A study of agglomeration between highly insulating particles should consider not only the initial agglomeration induced by the micro fields, but also adhesion caused by the persistence of these fields after the particles are in contact.

APPENDIX

To solve Eqs. (III.18) to (III.21), substitute (III.18) solved for q_2 into (III.21) to obtain a single, second-order equation in $n_1(x)$:

$$\frac{d}{dx}\left[\frac{1}{n_1}\ \frac{dn_1}{dx} + \frac{1}{\ell^*}\frac{n_1}{n_1(0)}\right] \ = \ 0 \qquad \text{(A.1)}$$

The quantity in brackets is a constant determined by the initial conditions. To evaluate the first term at $x = 0$, Eq. (III.18) is used, together with the definitions of (n,ℓ^*) following (III.23). Thus,

$$\frac{1}{n_1}\ \frac{dn_1}{dx} + \ \frac{n_1}{\ell^* n_1(0)} \ = \ \frac{-\eta}{\ell^*} \qquad \text{(A.2)}$$

To solve this expression, substitute $n = 1/V$, to get

$$\frac{dV}{dx} - \ \frac{\eta}{\ell^*}\,V \ = \ \frac{1}{\ell^* n_1(0)} \qquad \text{(A.3)}$$

This constant-coefficient expression has a particular solution $V = 1/\eta n_1(0)$ and homogeneous solution $C \exp(\eta x/\ell^*)$. The constant, C, is determined by the condition that $n_1(x=0) = n_1(0)$. So we get Eq. (III.22). The expression for $q_2(x)$, Eq. (III.23), is achieved from this result using (III.24).

REFERENCES

1. Sargent, G. D., "Dust Collection Equipment", Chem. Engineering, Jan. 27, 1969, pp. 130-150.

2. Allan, D. L., "The Prevention of Atmospheric Pollution in the Carbon Black Industry", Chemistry & Industry, Oct. 15, 1955, pp. 1320-1324.

3. Drogin, I., "Carbon Black", J. of the Air Poll. Control Assoc., 18, (1968), pp. 216-228.

4. Lunde, K. E., and Lapple, C. E., "Dust and Mist Collection - A Critique on the State of the Art", J. of the Air Poll. Control Assoc., 7, (1958), pp. 289-296.

5. Walker, A. E., "Enhanced Scrubbing of Black Liquor Boiler Fumes by Electrostatic Pre-agglomeration: A Pilot Plant Study", J. of the Air Poll. Assoc., 13, #12, December 1963, pp. 622-627.

6. Strubler, G., "Device for Agglomerating Microscopic Particles", U.S. Patent 3,110,580, April 14, 1960.

7. Strubler, G., "Electrostatic Agglomerator Having an Improved Discharge Electrode Structure", U.S. Patent 3,257,779, Sept. 15, 1961.

8. Lau, H., "AC Electrostatic Precipitator", Staub-Reinhalt. Luft 29, #8, August, 1969, pp. 10-13.

9. Szantho, E. V., "Agglomeration Dust in Smoke Flues", Staub-Reinhalt. Luft 29, #8, August 1969, pp. 6-9.

10. Fuchs, N. A., The Mechanics of Aerosols, Pergamon Press and MacMillan Co., Inc., New York (1964), p. 310.

11. Kraemer, H. F., and Johnstone, H. F., "Collection of Aerosol Particles in Presence of Electrostatic Fields", Industrial & Engineering Chem., 47, #12, pp. 2426-2434.

12. Whytlaw-Graz, R., and Patterson, H. S., Smoke: A Study of Aerial Disperse Systems, Edward Arnold & Co., London (1932).

13. Gillespie, T., "The Effect of the Electric Charge Distribution on the Aging of an Aerosol", Proc. Royal Soc. A 216 (1953), pp. 569-582.

14. Zessack, U., "The Coagulation of Mixed Dusts", Staub-Reinhalt. Luft 28, #11 (1968), pp. 53-60.

15. Robinson, M., "Turbulent Gas Flow and Electrostatic Precipitation". J. of the Air Poll. Control Assoc., M18, (1968), pp. 235-239.

16. Chattock, A. P., "On the Velocity and Mass of the Ions in the Electric Wind in Air", London, Edinburgh and Dublin Philos. Magazine & Journal of Science, Vol. 48, #294, Nov. 1899, 2F, pp. 401-421.

17. Woodson, H. H., and Melcher, J. R., Electromechanical Dynamics, Part III. Elastic and Fluid Media, John Wiley & Sons, Inc., New York, 1969, p. 776.

18. Velkoff, H. R., and Ketcham, J., "Effect of an Electrostatic Field on Boundary-Layer Transition", AIAA, 6, #7, (1968), pp. 1381-1382.